Contents lists available at ScienceDirect

Weather and Climate Extremes

journal homepage: www.elsevier.com/locate/wace





Wave setup estimation at regional scale: Empirical and modeling-based multi-approach analysis in the Mediterranean Sea

Tim Toomey ^{a,*}, Marta Marcos ^{a,b}, Thomas Wahl ^c, Miguel Agulles ^a, Alejandra R. Enríquez ^c, Angel Amores ^{a,b}, Alejandro Orfila ^a

- a Mediterranean Institute for Advanced Studies (UIB-CSIC), Esporles, Balearic Islands, Spain
- b Department of Physics, University of the Balearic Islands, Palma, Balearic Islands, Spain
- ^c Department of Civil, Environmental and Construction Engineering, National Center for Integrated Coastal Research, University of Central Florida, Orlando, FL, USA

ARTICLE INFO

Keywords: Wave setup Numerical modeling Empirical formulation Beach-face slope Spatial resolution

ABSTRACT

Wave setup is a physical process that induces a temporal increase of the mean water level due to wave dissipation by bottom friction and breaking in the surf zone, extending over tens to hundreds of meters in the cross-shore direction. Wave setup contribution to coastal sea level solely induced by wind and atmospheric effects can increase by more than 100% under extreme events and conditions favoring its formation. It is therefore crucial to consider this phenomenon when assessing sea-level-related coastal hazards. Previous studies estimated the wave setup effect by means of numerical modeling and empirical formulations at regional and global scale. Such analyses require either high computational capacity to implement high-resolution numerical models over large domains, and/or accurate information on coastal morphological features from global or regional databases. Although the Mediterranean Sea is a fetch-limited environment, waves generated from extra-tropical cyclones are powerful enough for wave setup to develop, and subsequently for a potential significant wave setup contribution to extreme coastal sea level. Through the use of both numerical and empirical methods, we investigate the uncertainty associated to wave setup representation on the frequency and magnitude of coastal extreme sea levels occurring on sandy beaches in the Mediterranean Sea. Wave setup values are compared at beach scale between process-based modeling and empirical approaches, showing highly variable results. We also quantify the impact of wave setup on return levels of coastal sea level extremes using reconstructed sea levels. We employ various methods to calculate the wave setup component. Results show high spatial dispersion, with clear differences between the numerical and empirical approaches, especially in regions prone to the development of energetic waves. The total inter-method dispersion of 100-year return levels is often higher than 30 cm for average values of 62.4 cm. We emphasize the important limitations related to wave setup modeling (i.e., its underestimation) at large scale, and call for caution when applying empirical formulations (generally developed from local studies) at regional to global scale, which can lead to unrealistic wave setup values.

1. Introduction

Coastal extreme sea levels occurring during stormy meteorological conditions have been widely investigated at global and regional scales (Marcos et al., 2009; Vousdoukas et al., 2016, 2017; Wahl et al., 2017; Fernández-Montblanc et al., 2020; Muis et al., 2020; Melet et al., 2018, 2020). Such events are mainly driven by storm surges, defined as the elevation of the sea surface with respect to the predicted tide. Storm surges drivers are almost systematically reduced to the inverse barometric effect (associated to low atmospheric pressure) and wind setup effects, assuming wave setup induced by nearshore breaking

waves and bottom friction dissipation as an external contribution to the total water level. Similarly, swash (water uprush and backwash after a wave breaks) is often neglected. While the swash time frequency is typically associated with the individual wave periods, the wave setup component is more aligned with the average behavior of the wave field over extended periods, with a time frequency of the order of minutes to hours. In this work we focus on the wave setup effect on coastal extreme sea levels. In the Mediterranean Sea, the contribution of wave setup to coastal sea level is expected to be small compared to regions prone for swell generation and propagation, mostly because of limited

E-mail address: tim.toomey@uib.es (T. Toomey).

^{*} Corresponding author.

fetches. However, several studies focusing on coastal extreme sea level at hourly frequency showed that extra-tropical cyclones can produce high and powerful waves that eventually generate substantial wave setup, whose contribution to coastal sea level may be comparable in magnitude to other processes, such as wind setup and inverse barometer effects (Amores et al., 2020; Pérez-Gómez et al., 2021; Toomey et al., 2022b,a).

As introduced by Longuet-Higgins and Stewart (1964), the dissipation of waves propagating towards the coast can ultimately lead to the development of wave setup along the coast. Specifically, the waves dissipation in the nearshore induces horizontal variations of the radiation stress, i.e horizontal variations of transport of waveinduced momentum. Until the wave breaking point, wave-induced stress radiation increases due to wave shoaling, balanced by a negative mean surface slope (wave setdown). The wave radiation stress then decreases due to the wave dissipation by bottom friction and mainly wave breaking, balanced by a positive mean surface slope (wave setup). The radiation stress (RS) theory from Longuet-Higgins and Stewart (1964) has been previously employed in numerical simulations for characterizing the wave setup phenomenon. This has been achieved through the use of 2-dimensional horizontal (2DH) hydrodynamic model coupled with a spectral phase-averaged wave model. with several studies highlighting significant contribution of wave setup to coastal sea level (e.g., Roland et al. (2009), Bertin et al. (2015), Amores et al. (2020)). However, following the RS formalism, such 2DH approach cannot represent the vertical structure of the wave-induced circulation in the surf zone. Earlier studies (Guza and Thornton, 1981; Raubenheimer et al., 2001) stressed the potential underestimation of wave setup following Longuet-Higgins and Stewart (1964), especially at the shoreline. Apotsos et al. (2007) investigated the bottom stress owing to the mean offshore-directed flows in the surf zone (undertow). These authors showed that neglecting bottom stress could lead to severe underestimation of the wave setup (mean error 3 times larger for depths between 0.3 m and 1 m). In addition, Bennis et al. (2014) showed that accounting for both bottom stress and vertical mixing could significantly contribute to wave setup, later corroborated by Buckley et al. (2016). Specifically, these authors found a 16% wave setup increase due to bottom stress by reproducing in laboratory wave dissipation over a rough bottom mimicking a coral reef. Recently, using the SCHISM model (Zhang et al., 2016), Martins et al. (2022) investigated the impact of the depth-varying wave-induced mean circulation on wave setup through 3D fully coupled simulations with the vortex-force (VF) formalism of Bennis et al. (2011), first implemented by Guérin et al. (2018). They found that a 3D-VF approach accounting for waveinduced mean circulation in the surfzone could substantially increase wave setup. Specifically, for steep slopes (higher than 1:10), results from this study indicate an increased wave setup up to 30% compared to a 2DH-RS approach. When 3D simulations are not conceivable, Martins et al. (2022) also advocates 2D simulations with VF formalism that partly accounts for the onshore-directed bottom shear stress driven by the offshore-directed undertow. As a difference, the evaluation of the bottom stress is performed using the depth-integrated undertow current instead of the near bottom velocity and a Manning coefficient instead of the bottom roughness. As a result, the 2DH-VF simulations resulted in an increase of 10%-20% of wave setup compared to values from the 2DH-RS simulations (see for instance their Fig. 7c,d). Previously, using a VF formalism, Lavaud et al. (2020) reported very modest wave setup differences between results from 2DH and 3D modeling, with both improvement and deterioration of wave setup values, the latter being in part attributed to the limited spatial resolution (up to ~ 35 m). Also, in contrast with study sites from Martins et al. (2022) where significant wave setup increase is observed following a 3D approach, the zones investigated by Lavaud et al. (2020) (Arcachon Lagoon and Adour Estuary, France) are characterized by much gentler slopes (1:50 to 1:100), limiting the influence of the 3D approach and highlighting the important role of the varying bed slopes for wave setup representation.

From regional to local scale, several works have focused on the contribution of wave setup to coastal sea level, based on numerical modeling (Bertin et al., 2015; Amores et al., 2020; Lavaud et al., 2020; Toomey et al., 2022a; Agulles and Jordà, 2023), in-situ and remote data (Pedreros et al., 2018; Ray et al., 2022; Abessolo et al., 2023). Since the spatial scale of wave setup imprint on the coast extends from tens to hundreds of meters in the cross-shore direction, the associated spatial resolution needed to simulate this physical process demands high computational efforts when performed at regional and global scale. Furthermore, the formation of wave setup is strongly dependent on morphological features. Indeed, coastal areas characterized by narrow continental shelves (e.g. volcanic islands, Kennedy et al. (2012)) can often witness coastal sea level dominated by atmospheric pressure and wave effects along with a weak wind setup, while the latter is dominant in dissipative sandy beaches with mild slopes and located over a wide and shallow shelf. Also, the typology of the bottom can induce differences in wave dissipation due to bottom friction. Therefore, accurate information on both nearshore waves and morphological characteristics of the area of interest are necessary for wave setup representation. A widespread alternative approach consists of representing wave setup through empirical formulations (e.g., Melet et al. (2018, 2020), taking advantage of global wave models (e.g., Hemer and Trenham (2016)) and datasets providing information on coastal morphological features (e.g., Wolff et al. (2018)). As an example, Almar et al. (2021) calculated the maximum wave runup applying (Stockdon et al., 2006) formulation, and even coastal overtopping at global scale, using the General Bathymetric Chart of the Oceans (GEBCO, 400 m spatial resolution, https://www.gebco.net) and a global digital surface model (30 m resolution, ALOS Global Digital Surface Model, (Tadono et al., 2016)). The application of empirical formulations that have been validated only with local in-situ observations for regional and global scale analyses is quite straightforward, but requires continuous data as inputs, and is usually uniformly applied regardless of the coastal morphological variability (e.g. assuming a unique typology). On the other hand, the dynamical simulation of wave setup using hydrodynamicwave coupled models can overcome such limitations. Nonetheless, it is limited by the scale of analyses, forcing to adopt a 2DH approach over a 3D approach, and the required spatial resolution. Taking advantage of a recent model-based 72-years hindcast of coastal sea level including wave setup effect in the Mediterranean Sea (CoExMed dataset, Toomey et al. (2022a)), the overall objective in this work is to characterize, at regional scale, the contribution of wave setup to coastal extreme sea levels and its representation through numerical modeling and empirical formulations, along with the uncertainty associated to such multiapproach analysis. Doing so, the swash component is neglected and therefore the wave contribution to coastal extreme sea levels is only partly represented. Further, the role of angle of approach of the method used to represent the wave setup is also investigated. To do so, the performance of different methods used to represent the wave setup effect from a regional perspective is evaluated against methods used to derive wave setup at local scale, for three beaches located in Spain for which in-situ measurements are available.

The paper is structured as follows: the different areas of study and data directly providing wave setup levels at regional and local scale are presented in Section 2. Additional approaches used for the quantification of the wave setup component are detailed in Section 3. Results are analyzed from two different perspectives: first, focusing on specific areas at local scale, the role of the spatial scale of application for empirical methods and coastal wave setup modeling is investigated in Section 4. Further, the computation of return levels of coastal extreme sea levels at regional scale and the associated impact of the wave setup approaches are presented in Section 5. Finally, the methods to represent wave setup at large scales along with the implications of omitting the swash component are discussed, and results are summarized in Section 7.

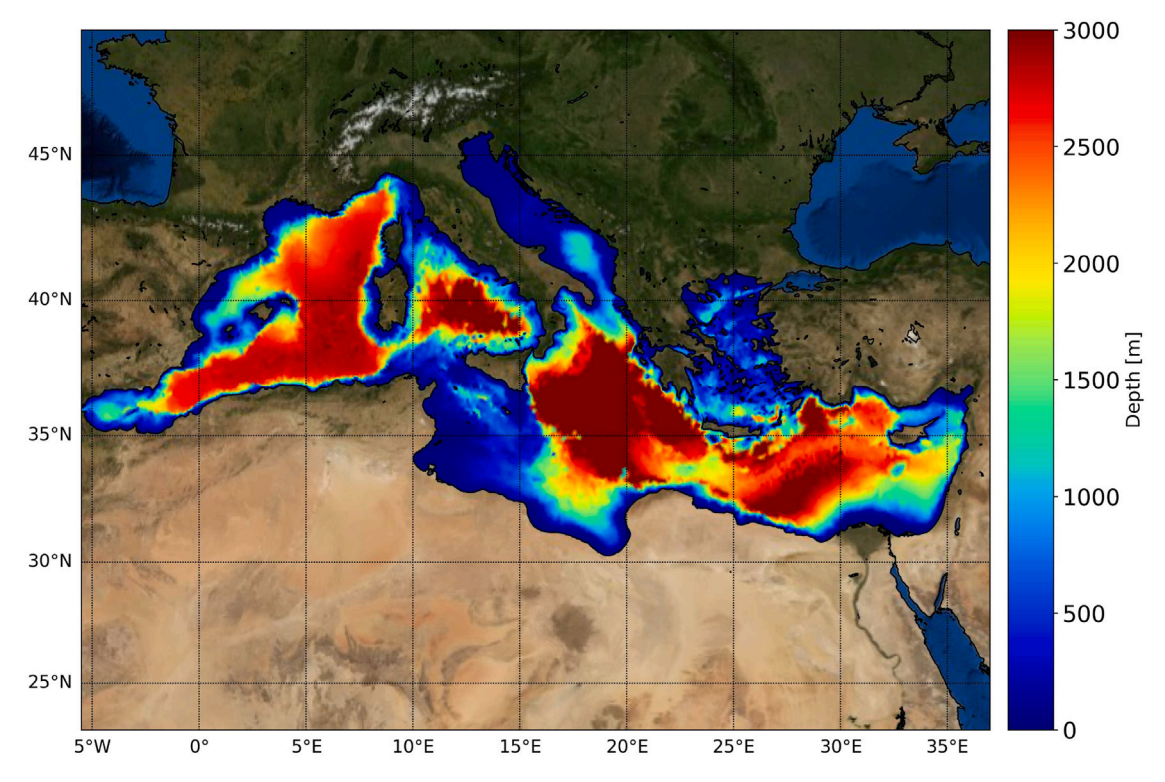


Fig. 1. Bathymetry of the Mediterranean Sea. *Source:* From CoExMed dataset.

2. Study region and ocean data availability

2.1. Areas of study

The Mediterranean Sea is a semi-enclosed basin connected to the Atlantic ocean through the Strait of Gibraltar. In part surrounded by mountains, the basin is characterized by its complex orography, channeling regional winds (e.g. Tramontane, Mistral, Sirocco) and comprises several interconnected seas with their own ocean dynamics (e.g. Adriatic sea, Medugorac et al. (2018)). Throughout this work we will analyze the entire Mediterranean coastline (see Fig. 1), islands included, which provides a very rich body of geomorphological features (different widths of the continental shelf, orientations, slopes, sediment types, etc ...) and a variable shallow-water dynamics driving local sea level variability (Section 5.2). Then, the area of study is narrowed down to the sandy beaches (see Fig. 2) of Playa de Palma (PDP, Fig. 2F) and Cala Millor (CLM, Fig. 2G), both located in the Mallorca island (Spain, Balearic Islands), and the beach of Gandia (Fig. 2G), located in the south of Valencia (Spain).

2.2. Sea surface elevation and wave data

We have performed a series of experiments to evaluate wave setup in three case studies. These experiments include data from a regional hindcast (CoExMed), a local hydrodynamic model (XBeach), and empirical formulations (Stockdon). These models and empirical formulations have been forced with in-situ observations and the previously mentioned hindcast. These experiments are further explained below.

2.2.1. Regional hydrodynamic-wave hindcast: CoExMed dataset

The CoExMed dataset generated by Toomey et al. (2022a) provides a high-resolution sea surface elevation and wave hindcast of the Mediterranean Sea, with an unstructured grid and a spatial resolution of ~ 20 km in the open sea down to ~ 200 m at the coast. The EMODnet (Bathymetry, 2018), that provides a regular grid with a

 $1/16 \times 1/16$ arc minutes (~ 115 m × 115 m) horizontal resolution, was used. The CoExMed database was generated using the SCHISM model (Zhang et al., 2016), a fully-coupled hydrodynamic and wave model, forced with hourly fields of wind (at 10 m above sea level) and pressure at mean sea level from the ERA5 reanalysis dataset (Hersbach et al., 2020). Ocean variables (sea surface elevation, significant wave height $-H_s$ -, peak period $-T_p$ -, and mean wave direction $-D_p$ -) are provided on an hourly basis and for the period from 1950 to 2021. The CoExMed dataset contains a total of 111561 coastal nodes. Toomey et al. (2022a) performed two numerical simulations: (1) hydrodynamicwave coupled simulation and (2) a purely hydrodynamic model run. For the simulation accounting for waves, the SCHISM model following a 2DH-RS approach was used. The wave setup component is extracted by calculating the difference between both runs. Furthermore, surface wind stress was originally computed using a bulk formula of the drag coefficient following Pond and Pickard (2013). As discussed by Toomey et al. (2022a) (see their section 5), sea surface stress can be calculated using a wind and wave dependent formulation. Doing so, Bertin et al. (2015) (see also (Pineau-Guillou et al., 2020)) showed that under young and rough sea state conditions, the use of a wave dependent surface stress results in a more accurate modeling of waves and sea surface elevation. As an extension of the work carried out by Toomey et al. (2022a), we updated the CoExMed dataset with another simulation replacing the (Pond and Pickard, 2013) bulk formula with the wave dependent surface stress formulation described in Bertin et al. (2015). Here, the impact of the representation of sea surface stress is negligible (see section 5, Toomey et al. (2022a)) and it is not within the scope of this paper to study its importance for single events as in, e.g., Bertin et al. (2015) and Pineau-Guillou et al. (2020). However, for the sake of consistency, we follow Bertin et al. (2015) and Pineau-Guillou et al. (2020) recommendations for a semi-enclosed sea such as the Mediterranean Sea characterized by limited fetch and young sea states; thus, all SCHISM-originating data used in this work were generated using the wave dependent formulation for wind stress parameterization.

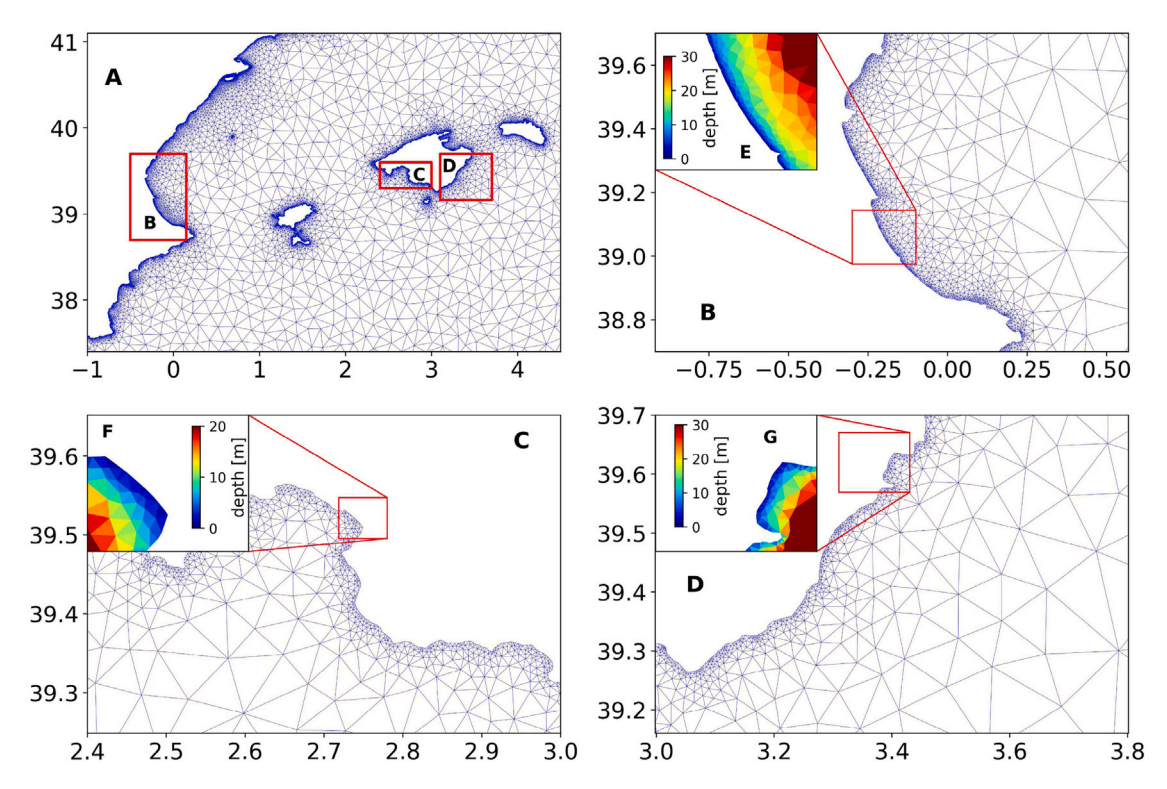


Fig. 2. CoExMed grid model around the Balearic Islands and eastern coasts of Spain (A). Zooms over the beaches of Gandia (B,E), Palma (C,F) and Cala Millor (G,D) are shown.

2.2.2. Local phase-resolving wave model

Wave setup modeling performance at regional scale will be compared to results from a local scale analysis carried out by Agulles and Jordà (2023). The authors computed the wave runup in PDP (from 2012 to 2017) and CLM (from 2011 to 2018) using XBeach, an opensource phase-resolving numerical model that simulates hydro- and morpho-dynamic processes on sandy coasts (Roelvink et al., 2015). The authors used high resolution topo-bathymetry from in situ field surveys and hourly nearshore wave observations (Tintoré et al., 2013) to feed the numerical model. As a result, both wave setup and swash component are provided. For both PDP and CLM beaches, the simulations horizontal resolution are 10 m and 2 m alongshore and cross-shore, respectively. To consider the bottom roughness, the authors used a Manning approach with a 0.025 coefficient, and a seagrass-dependent (Posidonia oceanica) vegetation module is used, playing a role on wave dampening and breaking, where vegetation fields are present (Ruiz-Fernández et al., 2015). The authors implemented the Xbeach model in both 1D and 2D modes. For the first case, the authors only selected events characterized by incident waves with direction of propagation inside a ±30° angle with respect to the cross-shore direction. Then, waves are assumed to propagate with normal direction to the coast, without directional spreading. Such approach implies the total transfer of offshore wave energy to the coast, which is not accurate in case of sea states characterized by a broad spectrum. Although the authors used nearshore observations of waves already refracted by the bathymetry, the total wave energy reaching the coast is overestimated (this point is further discussed in Section 6). Therefore, the available 2D simulations are used here instead, taking into account wave directional spreading. However, using XBeach in its 2D mode requires a very high computational cost and, therefore, a lower number of simulations were performed compared to the amount of 1D simulations. The authors selected an ensemble of 100 representative sea states using the kmeans algorithm to force their XBeach model, and reconstructed wave setup and swash time series through analogues identification method, following Camus et al. (2011). Every sea state is simulated during 40 min.

In addition to the simulations of local waves described above for PDP and CLM sites, using outputs of the CoExMed dataset, Toomey et al. (2022a) identified at regional scale areas with high contribution of the wave setup component to coastal extreme sea levels, such as the coastline around the Gulf of Valencia, characterized by a relatively wide continental shelf with shallow waters. For the sake of completion, the same methodology followed by Agulles and Jordà (2023) is applied at the beach of Gandia (Spain, Fig. 2E). The topo-bathymetric surveys are provided by IGN (Instituto Geográfico Nacional, https://www.ign.es/web/ign/portal) and the model is forced at its open boundaries with the outputs of the CoExMed dataset. Xbeach simulations are performed between 2012 and 2017, the same period as previous experiments on the beaches of CLM and PDP.

XBeach model outputs are considered here as the benchmark simulations because the model simulates the propagation and decay of individual waves and diagnoses wave setup directly, without any parameterization, unlike the other empirical approaches used in the work. We do not argue that XBeach is providing the "real" wave setup value, but only that, in absence of direct observations, it is our best approach at the local scale.

3. Empirical estimation of wave setup component

Wave setup values obtained from high-resolution numerical modeling described above are compared, at regional and local scale, with other methods widely used in the literature. Given the challenges of wave setup numerical modeling at large scale and the scarcity of wave setup observations, empirical and semi-empirical approaches have been commonly adopted to quantify the wave setup effect. For instance, the contribution of the wave setup to coastal sea level extremes at a global scale has been represented through the semi-empirical equation:

$$\bar{\eta} = kH_{\rm s},$$
 (1)

where $\bar{\eta}$ is the time-averaged wave setup and k a fixed coefficient. This formulation is assumed to be originated from the radiation stress theory developed by Longuet-Higgins and Stewart (1964) and leaning

on the assumption that the wave height at breaking depth (H_{br}) is equal to a fixed fraction of the local water depth (d_{br}) at breaking (constant breaker index, $\gamma = \frac{H_{br}}{d_{br}}$), as explained for instance in the Coastal Engineering Manual (see part II-4-3, Corps of Engineers (2002)) or Holthuijsen (2007) (see part 7.4.3). However, considering γ ranging from 0.5 to 1.5 and for a theoretical very steep beach slope of 1:12, the wave setup is approximated as (see 7.4.26 and 7.4.27 from Holthuijsen (2007)):

$$0.15H_{br} < \bar{\eta} < 0.45H_{br},\tag{2}$$

Note that H_{br} is the wave height at incipient breaking, and not the H_s at nearshore or offshore conditions as suggested in Eq. (1). Despite these vague approximations, equation (1), established for a steep slope, has been used to compute the wave setup contribution to coastal extreme sea levels with k=0.2 (e.g. Vousdoukas et al. (2017), Marcos et al. (2019)). In the present work, the impact of using such formulation for extreme sea level estimation at Mediterranean scale is further investigated. Moreover, Stockdon et al. (2006) proposed an empirical formulation to obtain the wave runup on natural beaches. The authors developed an independent formulation for the two processes driving the runup: the total swash-excursion and the time-averaged wave setup. The latter is defined as:

$$\overline{\eta} = 0.35\beta \sqrt{H_o L_o},\tag{3}$$

where β represents the beach face slope and H_o and L_o are the significant wave height and wave length at deep waters, respectively (calculated following Fenton and McKee (1990)). Stockdon et al. (2006) formulation was validated on natural beaches, and therefore generally not used in the presence of muddy seafloor, reefs or anthropogenic sea defense structures. Stockdon et al. (2006) formulation has been widely used in regional and global assessments of coastal sea level extremes (e.g. Stockdon et al. (2014), Atkinson et al. (2017), Melet et al. (2018, 2020), Kirezci et al. (2020, 2023)), as a way to account for the effect of waves. In order to compare the values derived from Stockdon et al. (2006) empirical formulation to those obtained by CoExMed data, we selected those coastal grid points corresponding to sandy coasts, to be consistent with the environment for which the empirical formulation was designed. To do so, we used a database that characterizes the coastal material in 4 different types for the whole Mediterranean basin for a total of 11 975 points: rock pocket beaches, mud, unerodible and sand Wolff et al. (2018). Fig. 3A shows the coastal typology for the CoExMed dataset in the Bay of Palma (Spain). At the Mediterranean scale, 35 648 out of 111 561 CoExMed nodes were classified as sandy coastal points. We will use these coastal regions for the comparison between empirical and numerical approaches.

A key parameter in the (Stockdon et al., 2006) formulation is the foreshore slope of the beach. Previous studies assumed a uniform slope at global or regional scale (Melet et al., 2018, 2020; Kirezci et al., 2020, 2023). Likewise, we considered here constant slopes with values of 0.04 ($\beta_{0.04}$) and 0.1 ($\beta_{0.1}$), thus neglecting the spatial variability of coastal morphology. We also retrieve realistic values of foreshore slopes (β_{local}) for the Balearic Islands from Agulles et al. (2021). The authors exploited high-resolution data from the MITECO1. They obtained the beach slopes, following the methodology proposed by Bernabéu et al. (2001) and described in Agulles et al. (2021). Specifically, the slope around the swash zone is extracted from equilibrium profiles that are derived using the characteristic grain size D_{50} mm of each beach and the corresponding wave climate. As an example, Fig. 3B shows the distribution of beach slope for sandy coastal points in the Balearic Islands (Western Mediterranean). In PDP and CLM beaches, such methods yielded beach slopes of 0.0335 and 0.051, respectively. Using swash observations at these locations, Agulles and Jordà (2023) found similar

slopes (0.027 and 0.044) computed averaging the slope over a region $\pm 2\sigma$ around the swash zone (σ being the standard deviation of the continuous water level record). A beach slope of approximately 0.027 is found at the beach of Gandia from the topo-bathymetric surveys previously mentioned.

4. Limitation of wave setup representation: from regional to local scale

Wave setup from numerical simulations performed with the phaseresolving XBeach model for the three local cases are compared with the different approaches previously discussed (i.e, the empirical approaches and the modeling outputs from Xbeach and CoExMed). Wave setup values inferred from Stockdon et al. (2006) formulation are calculated using the constant beach slopes and the distribution of local slopes (β_{local}). In PDP and CLM β_{local} data from Agulles et al. (2021) were used, as these values are consistent with those derived directly from in-situ observations. For the beach of Gandia, local beach slope β_{local} is obtained from the topo-bathymetric survey. For each beach, five independent events are selected from Xbeach simulations wave setup time series. The independency of events is ensured by selecting local peaks with a three-day time-independent window (Cid et al., 2015; Vousdoukas et al., 2016). The resulting wave setup values for every approach are presented in Fig. 4 for the beaches of Gandia (A), PDP (B) and CLM (C). The results include the modeling outputs $\mu_{CoE \times Med}$ from Xbeach and CoExMed (indicated as $Xbeach_{\beta_{local}}^{H^{Coll}_{s}}$ $Xbeach_{\beta_{local}}^{H_{Alwac}^{Alwac}}$ in PDP and CLM, CoExMed wave setup values), and three cases of the (Stockdon et al., 2006) formulation: one with the local slope and wave forcing from CoExMed dataset in the beach of Gandia ($Stockdon_{\beta_{local}}^{H^{CoExMed}}$), two from in-situ wave data and local slope ($Stockdon_{\beta_{local}}^{H^{Auwac}}$) in PDP and CLM, and two others forced with CoExMed wave parameters and 0.04 and 0.1 slopes ($Stockdon_{\beta_{0.04}}^{H_0^{CoExMed}}$ and $Stockdon^{H^{CoExMed}_s}_{\beta_{0.1}}$, respectively). Note that in-situ wave observations (from AWAC) are favored as the wave input source in the Stockdon formulation when using a local slope ($Stockdon_o^{H_s^{Awac}}$). Conversely, in cases where constant slopes are chosen at the regional scale, the CoExMed wave climatology is employed as input wave data $(Stockdon_{\beta_{0,01}}^{H^{CoExMed}})$ and $Stockdon_{\beta_{0,1}}^{H^{CoExMed}})$.

Fig. 4 represents the five wave setup events at every beach. Al-

Fig. 4 represents the five wave setup events at every beach. Although only in-situ observations of wave setup could ideally be considered as "ground truth", given the scarcity of these measurements, we use our local modeling approach with XBeach as our benchmark results to which all other approaches are compared. In doing so, overall, wave setup levels from $Stockdon_{\beta_0}^{H^{CoExMed}}$ significantly exceed those from other sources. Specifically, maximum values are 2, 2.2 and 4.3 times greater than values inferred from Xbeach simulation in Gandia, PDP and CLM, respectively. When excluding $Stockdon_{\beta_{0.1}}^{H^{CoExMed}}$ formulation, results show a notable degree of heterogeneity between each site.

Regardless the method to represent wave setup, highest values are found for the beach of Gandia, where highest and most powerful waves are found among the three beaches studied. Specifically, $Stockdon_{\beta_{log}}^{H^{CoexMed}}$ displays wave setup values that closely align with $Xbeach_{\beta_{local}}^{H^{CoexMed}}$ results, except for the maximum value, for which $Stockdon_{\beta_{log}}^{H^{CoexMed}}$ provides a value closer to benchmark: 44 cm, 35 cm and 25 cm for $Xbeach_{\beta_{local}}^{H^{CoexMed}}$, $Stockdon_{\beta_{loo4}}^{H^{CoexMed}}$ and $Stockdon_{\beta_{local}}^{H^{CoexMed}}$, respectively. Furthermore, CoExMed wave setup data registers values lower than with other methods, displaying maximum value less than half as derived from Xbeach simulations. However, CoExMed maximum values are as high as 20 cm, showing the regional hindcast's ability to capture a noticeable wave setup effect in this beach in comparison with CLM and PDP. For the beaches of PDP and CLM, empirical approaches

^{1 (}https://www.miteco.gob.es/es/costas/temas/proteccion-costa/actuaciones-proteccion-costa/illes-balears/default.aspx)

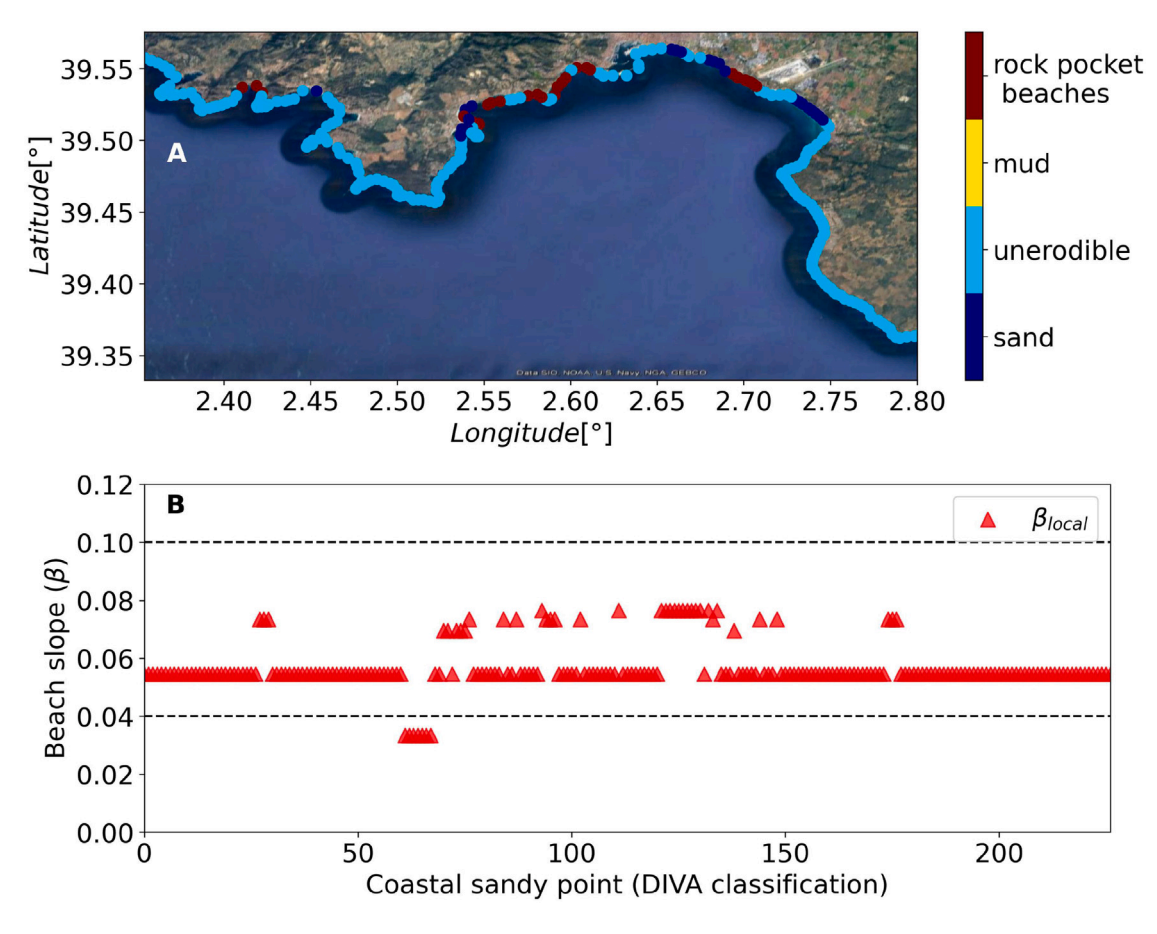


Fig. 3. Top panel: Bay of Palma (Google Earth image). Dots represent CoExMed coastal grid points and the associated coastal material type according to DIVA database classification. Bottom panel: Distribution of beach slopes from Agulles et al. (2021) for coastal sandy points located in the Balearic Islands (Spain). Dashed lines indicates the $\beta_{0.04}$ and $\beta_{0.1}$ slopes values.

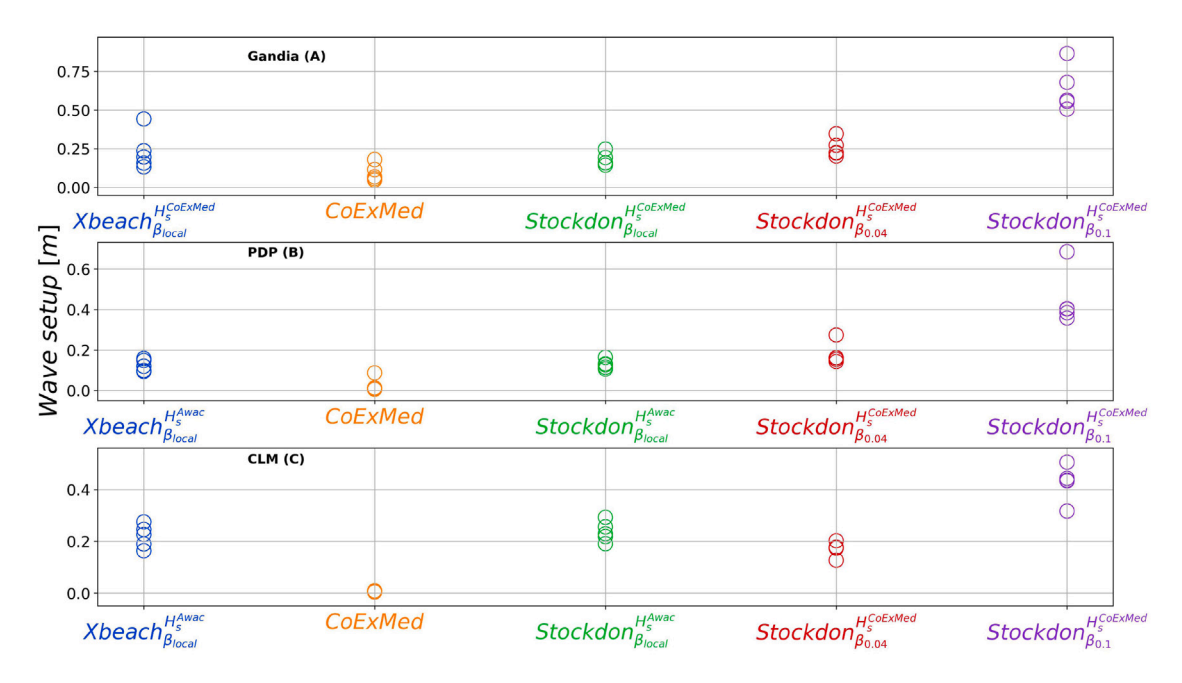


Fig. 4. Wave setup levels of 5 independent events (see Section 4) that occurred between 2012 to 2017 for each study case, at the beaches of Gandia (A), PDP (B) and CLM (C). From left to right, wave setup values from $wave_{scup}^{Xbeach}$, $wave_{scup}^{CoExMed}$, $wave_{scup}^{Rous}$ and $wave_{scup}^{Rous}$ and $wave_{scup}^{Rous}$.

results in similar or successively lower and higher wave setup levels than the Xbeach model. At PDP, maximum values are 15.8 cm, 16.4 cm and 27.4 cm for $Xbeach_{\beta_{local}}^{H^{SoexMed}}$, $Stockdon_{\beta_{local}}^{H^{Awac}}$ and $Stockdon_{\beta_{0.04}}^{H^{CoExMed}}$,

respectively. Likewise, at CLM, maximum values are 27.5 cm, 29.2 cm and 20.2 cm, for the same cases. It is noteworthy that we find clearly different values of the empirical approach $Stockdon^{H_s^{Awac}}_{\beta_{local}}$, with wave

setup values lower than 20 cm in PDP and higher than 20 cm in CLM. Both beaches show similar wave climate, with H_s values of 2.6 m and 2.93 m for PDP and CLM (in-situ data), respectively, corresponding to maximum wave setup events shown in Fig. 4. Wave setup levels inferred from Stockdon formulation are at first order driven by the beach slope value, and may underestimate or overestimate the benchmark wave setup value, independently from the wave input and depending on how well the local beach slope is represented. On the other hand, CoExMed clearly provides lower wave setup levels at PDP ($\overline{\eta} \le 8.7$ cm) and lower than 1 cm at CLM (i.e, no wave setup is captured), despite $Xbeach_{\beta_{local}}^{H_s^{Co.}}$ wave setup values being higher in CLM than in PDP. The latest is characterized by more dissipative conditions and a smaller slope than for CLM (Agulles and Jordà, 2023), that results, for a similar wave forcing, in lower wave setup levels simulated with Xbeach, whereas the contrary is observed for the CoExMed dataset. These results highlight the limitation associated to the computation of wave setup at the regional scale, with the numerical model not always being able to capture a clear wave setup imprint because of the spatial resolution, together with coastal depth inaccuracies. Specifically, in the CoExMed grid domain, its configuration has only 3 to 4 nodes between 20 m and the coastline in PDP and CLM; it is thus expected that the model has limited capacity to reproduce wave transformation processes up to the shore. Also, coastal nodes are characterized by depths lower than 50 cm and higher than 2 m in PDP and CLM, respectively. For the latter, only extreme waves can reach the necessary height for breaking to occur, and subsequently for wave setup to develop, since it is the most important process allowing its formation.

The impact of the model grid resolution alone on wave setup from the 2DH-RS approach has been explored more in detail. To do so, we produced a new simulation with the same regional numerical model as CoExMed and the same forcing but with much higher spatial resolution in the area of PDP (see Appendix A for more details), for one wave event that occurred on 2013-01-20 at 2 h (UTC+1). The only model setup difference between both configurations is the spatial node density, that is highly increased for the downscaling, as shown in Figure A.9 A (Downscaling) and B (CoExMed). The sea surface elevation, which includes the atmospheric surge and the wave setup effect (elev^{coupled}), along four cross-shore transects are shown in Figure A.9 C, D. In the downscaled case, elev^{coupled} is substantially higher close to the shoreline, with values reaching up to ~ 64 cm. This is 23% larger than for the coarser resolution for which the maximum coastal elevation is \sim 52 cm. The successive wave set-down and wave setup is observed on both panels C and D of Figure A.9, with a more pronounced effect for the downscaled configuration that tends to better represent this physical process because of the higher node density.

Overall, adopting a regional-scale methodology for representing wave setup can result in significant variability when compared to beach-scale approaches. In fact, it is very likely that the outputs from the CoExMed dataset underestimate wave setup values or do not even capture the processus imprint, whereas an empirical approach like the Stockdon formulation can yield diverse results, with the extent of underestimation or overestimation depending on the slope parameter and how close it is to the real local beach slope.

5. Return levels of coastal extreme sea levels using multiple approaches for the wave setup component

In this section, the resulting wave setup values calculated using the different methods are investigated in terms of their contribution to return levels of coastal sea level extremes obtained from every approach at regional scale. We first describe how return levels are computed in every approach and then discuss the differences among the results.

5.1. Computation of return levels

Prior to the computation of return levels, we build the time series of sea surface elevation accounting for wave setup using the different numerical and empirical approaches described above. From CoExMed simulation, we use sea surface elevation from the hydrodynamic wave-coupled model run ($elev^{coupled}$). For the empirical approaches, we use sea surface elevation from the hydrodynamic-only run ($elev^{hydro}$) and add the wave setup following the methods described in Section 3:

$$elev^{0.2H_s} = elev^{hydro} + 0.2 \times H_s,$$

 $elev^{\beta_{0.04}} = elev^{hydro} + 0.35 \times 0.04 \sqrt{H_s L_o},$
 $elev^{\beta_{0.1}} = elev^{hydro} + 0.35 \times 0.1 \sqrt{H.L.}.$ (4)

It is important to remark that the values of wave parameters are obtained from the extreme events identified with $elev^{coupled}$.

To compute return levels, we follow (Toomey et al., 2022a) and extract local peaks from the time series of $elev^{coupled}$ at every coastal grid point classified as sedimentary coast. To ensure independence of events we use a three-day time window. Then, extreme events are selected using the "Automated threshold selection technique" proposed by Thompson et al. (2009), developed from Coles (2001) method based on the stability of Generalized Pareto Distribution (GPD) scale and shape parameters. Toomey et al. (2022a) summarized (see their section 2.3) and applied this procedure to calculate extreme sea levels and H_s return levels (see section 2.1 of Thompson et al. (2009) for more details). As a result, a distribution of $elev^{coupled}$ extreme events is obtained as well as the simultaneous associated wave parameters (H_s , T_p , D_p) and $elev^{hydro}$. Return levels are then computed for $elev^{coupled}$ and for the three empirical approaches.

One example of the resulting time series is illustrated for a single point in Fig. 5A for a 4 month time period at a coastal point located in the Gulf of Valencia (east coast of Spain). Fig. 5A includes elev^{coupled} and elevhydro time series of extreme events, along with the corresponding reconstructed $elev^{0.2H_s}$, $elev^{\beta_{0.1}}$ and $elev^{\beta_{0.04}}$. In this example, it is evident that $elev^{0.2H_s}$ values are much higher than any other reconstructed or simulated sea surface elevation, and so will be the return levels. Moreover, $elev^{\beta_{0.1}}$ is always higher than $elev^{coupled}$ except for the local peak corresponding to the Gloria storm in 2020 (Amores et al., 2020), showing that the simulated wave setup is not purely proportional to a quantity involving wave bulk parameters as is it for the Stockdon's formulation (where $\bar{\eta}$ is proportional to $\sqrt{H_s L_a}$). Indeed (Stockdon et al., 2006) wave setup formulation is only dependent on the local slope β , H_s and T_p , but it does not take into account, for instance, the wave direction, in contrast to the results of numerical modeling, which likely explain the temporally variable differences and the fact that the corresponding return level curves (Fig. 5B) cross for return periods higher than 80 years. This point is further discussed in Section 6. We fit a GPD to each distribution of extreme events and compute return levels for periods of up to 200 years at every sandy coastal grid point.

5.2. Impact of the wave setup approach on return levels of coastal extreme sea levels

Return levels of coastal extreme sea levels using the different approaches to account for wave setup have been computed for the 35648 coastal grid points corresponding to sandy coastal regions in the Mediterranean basin. as an example, Fig. 5B shows the return levels for the same coastal point in the Bay of Valencia used in Fig. 5A. As expected from the amplitudes observed in Fig. 5A, return level curves show different behavior. The highest return levels in comparison to all other methods are obtained for $elev^{0.2H_s}$. Indeed, the 1-year $elev^{0.2H_s}$ return level is higher than any other 200-year return levels of extreme sea levels, suggesting that this approach results in unrealistic values. Among the other curves, simulated $elev^{coupled}$ and $elev^{\beta_{0.1}}$ clearly show

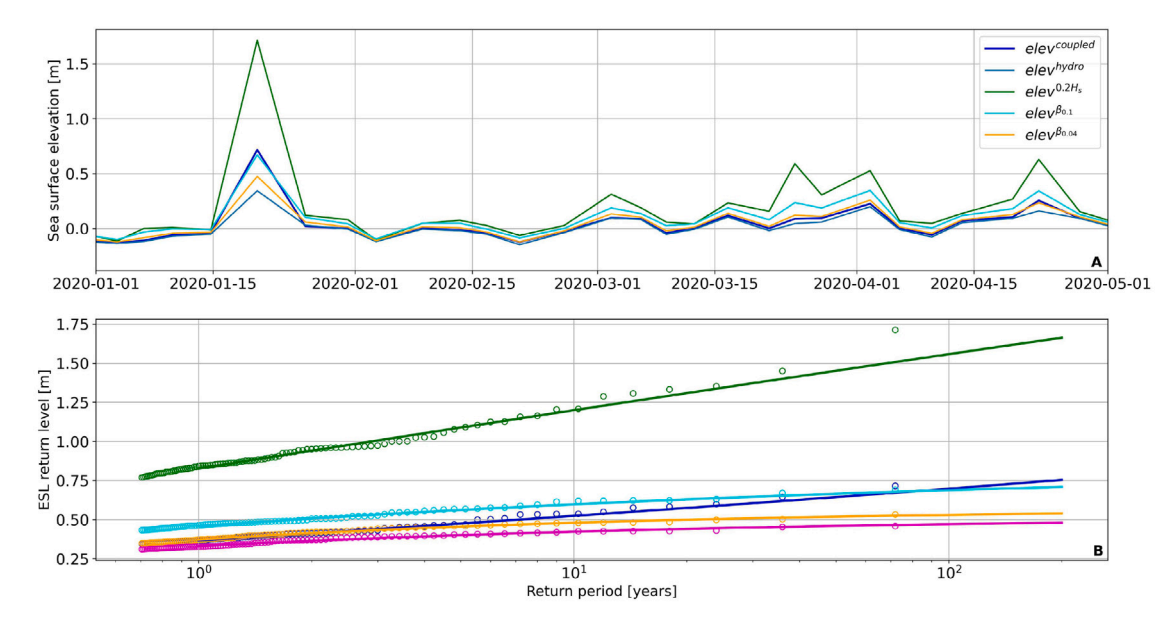


Fig. 5. A: Simulated ($elev^{coupled}$) and reconstructed extreme sea levels during independent events (declustered using a three-day time window) at a coastal point in the Gulf of Valencia (Spain). Reconstructed time series include $elev^{hydro}$, $elev^{0.2H_s}$, $elev^{\theta_{0.1}}$ and $elev^{\theta_{0.04}}$. Wave bulk parameters are extracted at 30 m depth. B: Return levels of sea level extremes at a coastal point in the Gulf of Valencia for $elev^{coupled}$, $elev^{hydro}$, $elev^{0.2H_s}$, $elev^{\theta_{0.1}}$ and $elev^{\theta_{0.04}}$.

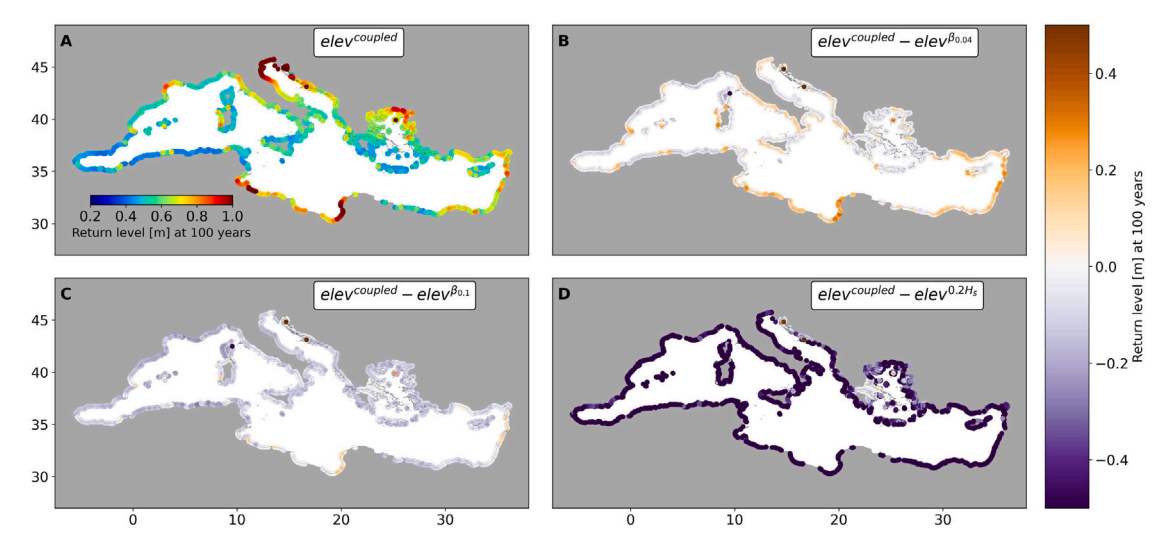


Fig. 6. A: 100-year return levels of $elev^{coupled}$ computed from CoExMed output. Other panels show the differences in 100-year return levels between $elev^{coupled}$ and reconstructed extreme sea levels from the combination of $elev^{hydro}$ and wave setup values following Stockdon's formulation with $\beta_{0.04}$ (B), $\beta_{0.1}$ (C) and $0.2H_s$ formulation (D).

highest return level at this specific coastal point. As mentioned earlier, for return periods lower than 80 years, $elev^{\beta_{0.1}}$ return levels are higher than $elev^{coupled}$, but both curves cross afterwards. As first observed in Fig. 5A, $elev^{coupled}$ is higher than $elev^{\beta_{0.1}}$ during most extreme events and lower for weaker events. Moreover, the other methods yield lower 1 to 200-year return levels than $elev^{coupled}$.

For the purpose of representing the results for all coastal grid points, we focus on 100-year return level, taking as reference the values obtained with $elev^{coupled}$. Fig. 6 maps the 100-years return level of $elev^{coupled}$ (A) and its differences with $elev^{\beta_{0.04}}$ (B), $elev^{\beta_{0.1}}$ (C) and $elev^{\beta_{0.2}H_s}$ (D) 100-year return levels. Note that the total number of sandy coastal points is very high (35 648 nodes) and representing them all on a single map inevitably leads to overlapping points. The values in Fig. 6D are consistent with those in Fig. 5B, showing that $elev^{0.2H_s}$ return levels exceed those from $elev^{coupled}$ almost everywhere in the Mediterranean Sea, except for fully fetch-limiting areas in the gulfs of Corinth and Eubeoa in eastern coasts of Greece. Indeed, for 87.7% (68.8%, 22.4%) coastal sandy grid points, 100-year $elev^{0.2H_s}$ return

levels are at least 25 cm (50 cm, 80 cm) higher than 100-year elev^{coupled} return levels. Other methods deriving wave setup from Stockdon et al. (2006) formulation result in closer values to elev^{coupled} return levels, though with some notable differences. In both cases, Figs. 6 B and C, display similar spatial patterns, which are also consistent with (Toomey et al., 2022a), showing higher values of elev^{coupled} in regions favorable to its development. There are well defined areas (Fig. 6A) where 100-year elev^{coupled} return levels can be equal or higher than elev^{0.04} return levels, such as the gulfs of Lions southwest of France, Gabes and Syrte (north of Lybia) and parts of the coasts of the Levantine or southern Sicily (Italy). Up to 4.3% coastal sandy points, mainly located in these areas, show 100-year elevcoupled return levels 10 cm higher than 100-year $elev^{0.04}$ return levels. Concerning $elev^{\beta_{0.1}}$, the 100year return levels are lower or equal to 100-year elev^{coupled} return levels at only 1.6% of coastal sandy point. Likewise, geographical zones where the hydrodynamic-wave coupled model yields lower sea level extremes than empirical methods are explicitly defined, such as the northern coasts of Algeria and Tunisia, eastern coasts of Spain (except

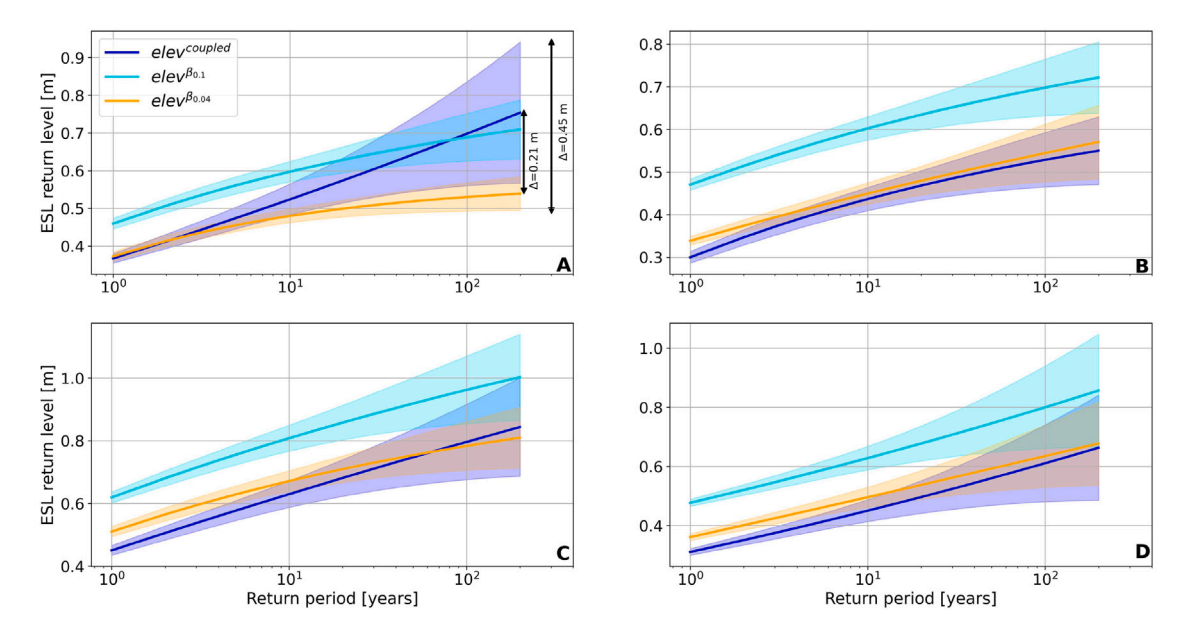


Fig. 7. Return levels of extreme sea levels at coastal points located in Valencia (Spain, A), Tel-Aviv (Israel, B), Gulf of Lions (France, C) and Gulf of Syrte (Libya, D), with the 95% confidence intervals shown in shadowed areas. The maximum dispersion is shown in panel A (Δ, in m) for 200-year return level and its confidence intervals.

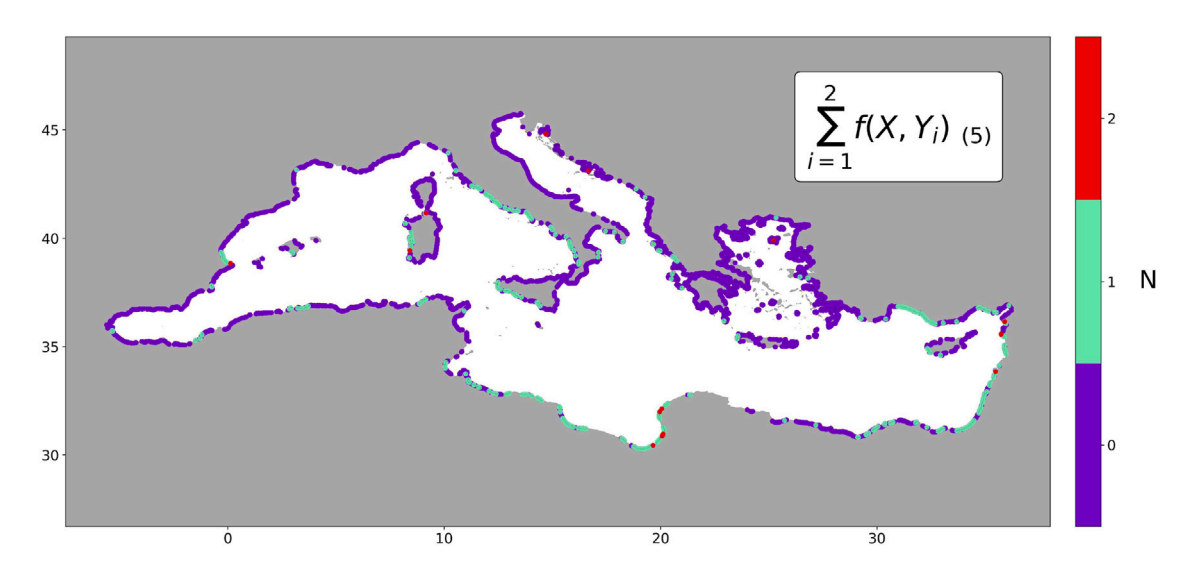


Fig. 8. Comparison between 100-year return levels of eleverapled and the uncertainties of the ensemble empirical approaches, according to Eq. (5) (see Section 5.2 for details).

the southern coasts of the Gulf of Valencia) or the eastern coasts of the Adriatic. In more detail, 8.8% and 75.8% of coastal sandy points show 100-year $elev^{coupled}$ that are at least 10 cm lower than 100-year $elev^{\theta_{0.04}}$ and $elev^{\theta_{0.1}}$, respectively. Similarly to $elev^{0.2H_s}$, such high percentage for $elev^{\theta_{0.1}}$ compared to other methods was expected, since beach slopes are generally smaller than 0.1 and such assumption can lead to overestimated wave setup. For instance, Melet et al. (2020) found global beach slopes ranging from 0.005 to 0.20 with a median value of 0.04 (see section 2.1.2) and Agulles et al. (2021) inferred beach slope values confined between 0.034 and 0.075 for the Balearic Islands.

We complement this analysis by looking at the return level dispersion, including the uncertainty associated to return level computation. For this evaluation we neglect the case of $elev^{0.2H_s}$, because of their much larger values. Fig. 7 shows return level curves for periods ranging between 1 and 200 years and for $elev^{coupled}$, $elev^{\beta_{0.04}}$ and $elev^{\beta_{0.1}}$. The lower and upper boundaries correspond to the 95% confidence intervals. Results are displayed at four different locations, representing contrasting areas: Gulf of Valencia (Spain, A), Tel-Aviv (Israel, B), Gulf of Lions (France, C) and Gulf of Syrte (Libya, D). Fig. 7 represents the

return level variability associated to different estimates of wave setup in sea surface elevation, which display distinct behavior at different locations. For return levels up to 200 years, there is no general rule on the method providing higher values (when $elev^{0.2H_s}$ is excluded), as the resulting elevations are dependent upon morphological patterns and wave power and directions, that are considered differently in the methods. The 100-year elevcoupled return level is the highest for the coastal point located near Valencia (A), whereas $elev^{\beta_{0.1}}$ return levels are significantly higher in Tel-Aviv (B) and in the Gulfs of Lions (C) and Syrte (D). Concerning $elev^{\beta_{0.04}}$, 1-year return levels are always greater than for elev^{coupled}. However for every case shown in Fig. 7, the higher the return period, the lower the difference between both curves, with a crossing around 3-year and 64-year return period at Valencia (A) and in the Gulf of Lions (C), respectively. In alignment with the previous comments on Fig. 5, these observations illustrate how the results, depending on the selection of the methodology to represent the wave setup contribution to coastal elevation, may diverge depending on whether we consider an isolated event, a return period of 1, 10, or 100 years. One way to quantify the multi-approach variability is to calculate the difference between the highest and lowest 100-year return levels among the three methods. For example, at the coastal grid point in the Gulf of Valencia, $elev^{\beta_{0.04}}$ and $elev^{coupled}$ provide the lowest and highest 200-year return levels, respectively, with a total difference of 21 cm. At the Mediterranean scale and a for 100-year return period, this dispersion is higher than 10 cm (20 cm, 30 cm) for 86.3% of coastal points (18%, 0.7%). Taking into account the total dispersion (i.e. the difference between lower and upper confidence interval boundaries), it is higher than 10 cm (20 cm, 30 cm) for 98.1% coastal points (31.7%, 6.1%). Such dispersion levels originating from wave setup representation are significant for the Mediterranean Sea, as $elev^{coupled}$ shows a median 100-year return level of 56 cm (88 cm for the 95th quantile). Indeed, for a dispersion higher than 10 cm (20 cm, 30 cm), the associated median relative dispersion (100 * $\frac{dispersion}{RL_{100}^{elev} coupled}$) is 35% (51.1%, 77.5%).

To assess the added-value of the hydrodynamic-wave coupling with respect to other parametric approaches, we compare the $elev^{coupled}$ with the two other methods, $elev^{\beta_{0.1}}$, $elev^{\beta_{0.04}}$, defining the following metrics for the 100-year return levels ($RL_{100year}$) and their uncertainty using the 95% confidence interval ($RL_{100year}^{95\%}$):

$$X = RL_{100year}^{elev^{coupled}}, \quad Y = RL_{100year}^{95\%} \begin{pmatrix} \beta_{0.1} \\ \beta_{0.04} \end{pmatrix}$$

$$f(X, Y_i) = \begin{cases} 1 & \text{if } X > Y_i \\ 0 & \text{if } X < Y_i \end{cases}$$

$$N = \sum_{i=1}^{2} f(X, Y_i) \tag{5}$$

where $\beta_{0.04},\ \beta_{0.1}$ correspond to $elev^{\beta_{0.1}},\ elev^{\beta_{0.04}},$ and N ranges from 0 to 2. Lower N values indicate that the 100-year return level computed using elev^{coupled} fall within the uncertainty ranges of other methods; for instance, if 100-year elev^{coupled} return level is higher than the upper confidence interval of 100-year $elev^{\beta_{0.04}}$ return levels and lower than upper confidence interval of 100-year $elev^{\beta_{0.1}}$ return level, N=1. Conversely, if N equals 0, it indicates that the return levels fall inside the confidence intervals of any other method. Note here that the confidence interval has been defined in a conservative way (higher likelihood of containing the results). The results for N at every coastal grid point are mapped in Fig. 8. Very similarly to Fig. 6, areas where $N \ge 1$ are well defined: gulfs of Gabes and Syrte, south bay of Valencia, eastern coasts of Sardinia, southern coasts of Sicily, coasts of the Levantine Sea, and the western coasts of Italy bordering the Tyrrhenian Sea. However, 100-year elev^{coupled} return levels are not significantly higher (N = 0) than return levels from other methods for 93.4% of coastal sandy grid points. Furthermore, N > 0 (N = 2) is found for only 6.6% (0.14%) of coastal points, mainly located along the previously mentioned geographical zones. Except for $elev^{\beta_{0.1}}$, results shown in Figs. 6 and 8 indicate that where the model captures a clear and significant wave setup imprint on the coast, it is likely to yield return levels higher than those inferred from the combination of simulated elevhydro and Stockdon et al. (2006) wave setup approach. We recall here that we discarded the formulation $elev^{0.2H_s}$, as it exceeds by far return levels calculated from any other methods almost everywhere in the Mediterranean basin and are thus considered unrealistic. On the contrary, along coasts where the model is not able to capture wave setup, either because the real conditions are not favorable for wave setup formation, or because the model setup is too coarse to resolve the physical processes involved and limited by a 2DH approach, elev^{coupled} return levels are systematically lower than return levels from the other methods. Indeed, at Mediterranean scale, 100-year elev^{coupled} return levels are lower than the lower boundary confidence interval of $elev^{\beta_{0.04}}$ 100-year return levels at 45.9% of coastal sandy points. Independently of the wave forcing and morphological features (e.g. wave direction, coastal typology), such empirical methods always add a wave setup contribution, regardless of being realistic or not.

Previous results show the high variability associated to the use of different methods to derive the wave setup component. However, our purpose is not to discard (Stockdon et al., 2006) formulation or hydrodynamic-wave coupled numerical simulations for wave setup representation, but to show that such methods are very dependent on the spatial scale of application.

6. Discussion

As demonstrated by the preceding findings, the characterization of wave setup on a large scale, as observed in the case of the Mediterranean Sea through various methodologies, either numerical or empirical, can result in a substantial degree of variability in the contribution of wave setup to extreme coastal sea levels.

The contribution of wave setup to extreme sea levels becomes relevant under energetic ocean wave conditions. This is the case, for example, of tropical cyclones propagating over long distances with sustained winds (large fetch), resulting in high waves. For instance, during Hurricane Katrina in 2005, significant wave heights greater than 16 m were recorded (Wang and Oey, 2008), and, coupled to strong wind setup effect, generated storm surges greater than 7 m (Fritz et al., 2007). In regions such as the Gulf of Mexico or the Mediterranean Sea, storm surges and wave setup are expected to be much lower, since wave generation and propagation is fetch-limited. However, the Gulf of Mexico is subject to the influence of tropical cyclones, a factor absent in the Mediterranean basin. Nonetheless, recent studies showed that high waves ($H_s > 8$ m) can lead to significant wave setup contribution to extreme sea levels (Amores et al., 2020; Pérez-Gómez et al., 2021) of several tens of cm in the Mediterranean. Also, the contribution of wave setup to extreme sea levels extends for relatively long coastal stretches (Toomey et al., 2022a). Wave setup contribution to extreme sea levels should therefore be accounted for when performing coastal hazards assessments in the Mediterranean, despite the associated limited wave growth. At the regional scale, the methodology employed greatly impacts the results: we found a large dispersion between wave setup representation from numerical modeling and empirical formulations considered in this work. In particular, using the commonly applied rule of thumb to estimate wave setup as $\bar{\eta} = kH_s$ with k = 0.2 leads to dramatic sea level extreme return levels, as shown in Section 5.2. Indeed, for 82.5% of coastal sandy points explored here, 1-year return levels computed using $elev^{0.2H_s}$ are higher than 100-year modeled return levels from elev^{coupled}; this reduces to 58.5% when compared to $elev^{\beta_{0.1}}$. This also confirms that using a beach slope of 0.1, overall leads to an overestimation of the sandy beach slopes in the Mediterranean Sea. Of course, such results are not surprising, especially considering the hypothesis leading to this semi-empirical approximation (see Section 3, Eqs. (1) and (2)). Even opting for a lower value of k, this simplistic formulation would yield very questionable results at the regional scale, since it does not consider the morphological environment neither the wave parameters other than the significant wave height. Also, our results indicate that the values of the wave setup contribution to extreme sea levels can be severely overestimated. We therefore do not recommend use the kH_s approximation with k = 0.2 to estimate wave setup for sandy beaches at the Mediterranean scale, or at least suggest a lower value of k. Nonetheless, such results should not discard the applicability of the latter formulation for smaller areas or at local scale, particularly in cases with distinct morphological configurations. For instance, wave setup behavior can significantly vary in regions characterized by rocky bottoms with abrupt changes in seabed. Recently, Ray et al. (2022) investigated coastal sea levels from satellite altimetry and a tide gauge located in Minamitorishima, a very small Japanese atoll in the western Pacific characterized by a steep reef. The authors found sea level differences between altimetric and coastal tide gauge data higher than 1 m, attributed to the breaking of waves (H_s lower than 5 m), and their results could be in some cases compatible with the

 $0.2H_{\odot}$ approximation. However, they found a near-linear dependence of wave setup with swell height only for one favorable direction. Figure 3 of Ray et al. (2022) illustrates the clear dependence of wave setup on the wave direction, with highest levels found for incident waves with direction normal to shore. Likewise, the wave direction proves to be of paramount significance in the context of wave setup formation when using hydrodynamic-wave coupled numerical model such as SCHISM. As an example, we consider the beach of Gandia, that is oriented at 60° according to nautical convention. Selecting the top 100 maximum wave setup events recorded in the CoExMed dataset spanning the period from 1950 to 2021, values ranging from 11 cm to 32 cm are associated with incident wave with a D_n of 60° (for 90 cases) and 45° (for 10 cases), corresponding to waves approaching normal to the shoreline. It is noteworthy that modeling accurately the wave peak direction T_n is limited by the spectral resolution (15° for the CoExMed dataset). In contrast to 2D numerical modeling, empirical formulations like the kH_s approximation or the (Stockdon et al., 2006) formulation, employed for the computation of the wave setup component, do not account for wave direction. Specifically, Stockdon et al. (2006) assumed a shore normal approach and reversed measured H_s from shoaled to deep water using linear wave theory, to provide comparable wave heights between all sites of the study, that showed varying conditions of measurements (e.g., wave buoys located at depths from 7 m to 20 m). Doing so, processes like local wave generation, friction, whitecapping, diffraction and refraction are neglected. The assumption on waves normal to coasts can be even more problematic here because the Mediterranean Sea is characterized by waves periods shorter than for coastal zones bordering large oceanic basins, that thereby refract less. In a recent study by Almar et al. (2021), a global analysis of extreme coastal water levels and its implication for potential overtopping was conducted, encompassing the wave runup effect, which combines not only the wave setup but also the swash excursion. The latter was calculated using the Stockdon formulation. The authors used wave inputs $(H_s \text{ and } T_n)$ sourced from the ERA-interim reanalysis (Dee et al., 2011), which features a spatial resolution of $0.5^{\circ} \times 0.5^{\circ}$, equivalent to 55 km at the equator and approximately 19 km at 70° latitude. Notably, wave direction was not incorporated in their analysis, assuming that all waves are refracted uniformly towards the shore, where the Stockdon formulation was applied. This approach results in an over-contribution of the wave setup component to coastal sea level, as it is consistently added irrespective of the offshore wave direction. Likewise, inaccurate wave direction is also a limitation for wave modeling, as sufficient spatial resolution and accurate bathymetric information are needed to reproduce waves refraction, along with the representation of features acting as shadowing and dissipative barriers such as small islands that can be handled through the use of unstructured meshes or methodologies accounting for unresolved obstacles (Mentaschi et al., 2020). We illustrate this argument with an example at the Bay of Palma (Mallorca Island) that is less than 20 km wide. At the bay entrance, highest waves (H_s) range from 3 m to 6 m (based on time series data extracted from the CoExMed dataset), with wave directions (D_n) varying from 165° to 300°. The beach of Palma (PDP) is oriented approximately at 228° and is open offshore in the directions between 197° to 250°. Thus, because of land shadow effect, not all incoming waves will experience refraction towards the shoreline with a perpendicular orientation, or even reach it. To mitigate the latter, Agulles and Jordà (2023) only selected sea states in which waves exhibited a direction within a range of $\pm 30^{\circ}$ perpendicular to the shoreline. Nonetheless, beyond considering wave direction alone, it is crucial to account for the directional spread of wave spectra, whether the wave inputs are referred to offshore locations or near the shoreline. The amount of energy transferred towards the coast varies significantly with the spectral width. Indeed, a broad spectrum transports only a fraction of its energy, whereas a narrow-band spectrum can transmit a larger part. However, whether using a 1D phase-resolving model or the empirical and semi-empirical formulations used in this study, the total amount of energy is assumed

to be transferred to the shore, irrespective of both the directional spread and wave direction, resulting in an overall overestimated wave setup effect. The latter is even exacerbated when deriving wave inputs from global wave models with relative low spatial resolution, from 1.5° to 0.5° (e.g. Vitousek et al. (2017), Rueda et al. (2017), Melet et al. (2018, 2020), Kirezci et al. (2020), Almar et al. (2021)), that do not accurately represent the morphodynamic features of the coastlines. Nevertheless, whether using empirical formulation or numerical modeling to assess coastal wave setup levels, both approaches are subject to different inaccuracies resulting from the process of wave propagation from offshore to nearshore areas.

Major concerns when estimating wave setup effect on a regional or global scale through empirical formulations are not only related to the wave input data but also the way morphological parameters are incorporated and, in particular, in the choice of the key parameter of beach slope. In the formulation proposed by Stockdon et al. (2006), the determination of the wave setup and swash components is critically dependent on the local beach slope. Given the absence of information on this parameter at large spatial scales, previous global scale studies assumed a constant value for the beach-face slope. Some are referred and discussed in Section 3 (Melet et al., 2018, 2020). Likewise, in an earlier study, with the objective of quantifying the increasing coastal flooding at global scale, Vitousek et al. (2017) estimated wave setup contribution to coastal water levels assuming dissipative beach conditions for the application of a beach slope independent Stockdon formulation $(\overline{\eta} = 0.016\beta\sqrt{H_oL_o})$. Essentially, this approach can be regarded as the selection of a constant slope value of ~ 0.046 in the original wave setup Stockdon formulation. Also, Kirezci et al. (2020) estimated wave setup component at global scale using a formulation dependent on deep-water wave steepness (H_{s0}/L_0) and bed slope from the Shore Protection Manual approach (Army Corps of Engineers, 1984), while also employing the Stockdon formulation for comparative purposes with consistent results. Following a sensitive analysis, a constant slope of 1/30 was selected (1/15 and 1/100 were also tested). Our findings obtained at the Mediterranean scale underscore the substantial uncertainty and the potential introduction of notable biases in extreme sea level estimation associated to this methodology that uses constant parameters for all coastal sectors and that requires a subjective choice for this value of the beach slope, often unrealistic.

It is worth highlighting that in the development and validation of the wave runup formulation proposed by Stockdon et al. (2006), the authors conducted a comprehensive analysis of data derived from ten field experiments. These experiments encompassed a range of observed beach slopes, spanning from 0.01 to 0.11. Some works have attempted to introduce this variability in the slope parameter. In the study conducted by Almar et al. (2021), the authors accounted for the extensive variability of beach-face slopes on a comprehensive globalscale. Following the methodology introduced by Diaz et al. (2019), the slope used as input parameter for the (Stockdon et al., 2006) formulation in Almar et al. (2021) was estimated as the average slope within the region determined by the shoreline and the inland distance given by the closest local maxima, specifically the dune top position. This value was retrieved from the ALOS Global Digital Surface Model (ALOS World 3D-30 m, Tadono et al. (2016)), referred to as AW3D30, that has a resolution of 1 arc-second (~ 30 m). Specifically, transects perpendicular to the coast were defined every 0.05° (~ 5 km), using the Global Self-consistent, Hierarchical, High-resolution Geography Database (GSHHS, Wessel and Smith (1996)) coastline "h" highest resolution (~ 1 km). Apart from the uncertainties associated to the wave inputs, which impact the estimation of wave setup and swash effects as discussed in the preceding paragraph, this methodology presents some additional limitations: first, the approach employed by the authors only considers the emerged part of the beach when estimating the beach-face slope, whereas as defined by Stockdon et al. (2006) should also encompass the submerged area (over a region $\pm 2\sigma$ around the waterline $\overline{\eta(t)}$, see Section 3). This can lead to different slope values. For example, Sánchez-Artús et al. (2023) investigated the vulnerability to erosion and flooding of a set of 55 beaches located in the Catalan coast (northwest of Spain). These beaches displayed an emerged beach slope ranging from 0.06 to 0.25, falling largely outside the range of beach slopes investigated in the study conducted by Stockdon et al. (2006). Additionally, Figure 5 from Almar et al. (2021) shows examples, specifically in the southwest of France and the Netherlands, where coastal slopes were computed over horizontal distance of 200 to 400 m, that are considerably larger compared to the $\overline{\eta(t)} \pm 2\sigma$ distance. In other regions with narrower beaches, common in the Mediterranean Sea, the AW3D30 dataset is much more limited. For instance, in the Balearic Islands, PDP and CLM are 30-50 m and 35-40 m wide, respectively (Agulles and Jordà, 2023). Second, regions displaying substantial tidal range can pose challenges for accurate coastline detection, in contrast with areas as the Mediterranean Sea characterized by a microtidal environment (Marcos et al., 2009). In their study, Almar et al. (2021) included tidal signals, but applied the (Stockdon et al., 2006) formulation independently of the tidal phase, whereas the wave setup and swash contributions to total water level can exhibit significant fluctuations during low or high tide conditions. Third, since (Almar et al., 2021) aims at assessing global wave runup contribution to coastal sea level from robust regional profile of coastal slopes, they averaged ten 0.05° (0.5°) spaced transects. While this approach may work for extensive, wide beaches, it very likely fails in our region of study. As an illustrative example, the southern coast of Mallorca stretches over 0.6°, with beach slopes ranging from 0.0335 to 0.0765 (Agulles et al., 2021) that leads to significant dispersion of wave setup contribution to coastal sea level, with levels equivalent to $\sim 50\% R L_{100~{\rm years}}^{elev^{coupled}}$ up to \sim $125\% RL_{100\ years}^{elev coupled}$. Finally, in addition to the wave setup component, Almar et al. (2021) calculated the swash component using the (Stockdon et al., 2006) formulation, which is also strongly sensitive to variations of the beach-face slope. It is worth noting that the validation of this formulation, as emphasized by the authors, is based on a limited set of moderate wave events. Consequently, the dependence of swash on beach slope amplifies the overall uncertainty associated with assessing the global impact of waves on coastal extreme sea levels. Although the swash component can locally pose a higher risk in terms of overtopping coastal defenses compared to the wave setup component alone, it must be remarked that this is a highly localized and high frequency process and that introducing this term at a regional or global coastal hazards assessment may introduce further uncertainties. Another example that attempts to incorporate local information of beach slopes was published by Rueda et al. (2017), who employed a site-specific beach slope to compute the wave setup component, using once again the (Stockdon et al., 2006) formulation. To do so, the authors estimated the beach slope using an empirical function of breaking wave height, period and the D_{50} mm, as proposed by Sunamurra (1984). They assumed a constant D_{50} of 0.25 mm, despite several studies have demonstrated significant variability in this parameter even within relatively small geographical areas. For example, Agulles et al. (2021) found D_{50} observed from 0.15 to 1 mm for beaches in the Balearic Islands, while (Sánchez-Artús et al., 2023) identified D_{50} ranging from 0.2 to 1.3 mm along the Catalan coast. To illustrate the impact of this variability, for a wave characterized by a breaking height of 2.5 m and a period of 8 s, the resulting slopes would be 0.06 and 0.038, for D_{50} values of 0.15 mm and 1 mm, respectively. One feature that the aforementioned studies have in common is that the wave setup component is computed via the Stockdon empirical formulation irrespective of the specific coastal typology, whereas this approach was designed and validated solely for sandy beaches, therefore introducing additional uncertainties when applied beyond this context. This constraint is also present when using numerical models at large spatial scales, owing to the inherent heterogeneity of seabed compositions, crucial for the representation of the bottom friction especially in shallow waters. For the generation of the CoExMed dataset, Toomey et al. (2022a) used a Manning approach with a 0.02 constant coefficient, uniformly

applied for the whole Mediterranean Sea. Yet, the nature of the seabed (e.g. sandy or rocky bottom) and the presence of vegetation (e.g. Posidonia oceanica meadows (Infantes et al., 2012)) can for instance induce additional wave attenuation and therefore also alter the outputs. Even provided consistent information on the nature of the seabed, the spatial resolution of the CoExMed grid is too coarse to account for small features such as localized submerged meadows. Likewise, the spatial resolution plays an important role to reproduce waves transformation processes leading to coastal wave setup (and set down), as shown by results exhibited in Figure A.9 with wave setup levels as twice higher when increasing the spatial resolution respect to the CoExMed dataset. Furthermore, independently of the approach followed to represent the wave dissipation in nearshore areas as explained in the introduction (RS and VF formalism), as well as the approximations employed for source terms in the wave action equation (e.g. triad interactions $S_{n/3}$), the scale of analysis and the associated spatial resolution strongly limits the representation of the wave setup through numerical modeling, with an overall substantial underestimation of wave setup contribution to extreme sea levels as indicated by results from Section 5.2. Finally, despite the approximations and limitations concerning the representation of wave setup and wave runup through empirical formulation as mentioned above, such approach permit the representation of the swash excursions, crucial for assessing the total wave contribution to coastal extreme sea levels, while it is not possible through 2D numerical modeling at regional or global scale.

7. Conclusions

The present work characterizes the wave setup contribution to coastal extreme sea levels along sandy coasts in the Mediterranean Sea using multiple approaches, including numerical modeling, empirical and semi-empirical parameterized formulations. Results from a coupled hydrodynamic-wave 2DH numerical model are compared to widely used empirical approaches. The comparison is performed first at local scale, for three different sandy beach located in Eastern Spain for which local bathymetric information is available, and, at Mediterranean scale in terms of 1 to 200-year return levels of sea level extremes in sandy beaches. We identify improvements and important limitations of numerical modeling at regional scale for the computation of the wave setup contribution which is significantly underestimated. Additionally, we provide evidence of substantial uncertainty and constraints associated with use of empirical methods at that scale. This study represents the first attempt, to our knowledge, of a comprehensive analysis of the contribution of wave setup to coastal extreme sea levels from regional numerical modeling together with empirically-based methods.

In the current study, in addition to a high-resolution numerical coupled hydrodynamic-wave model, we applied both empirical (Stockdon et al., 2006) and semi-empirical $(0.2H_s)$ methodologies to assess the wave setup contribution to extreme sea levels at both local and Mediterranean scale. At local scale, significant disparities emerge when estimating the wave setup component adopting either a local or a regional approaches. In summary, in comparison to benchmark values derived from a local simulation using a phase-resolving wave model, wave setup values obtained from the regional approach (CoExMed) consistently provides lower values than from other methodologies. Conversely, empirical approaches yield highly variable results depending on the local slope parameter and how well this is captured and introduced in the empirical formula. Furthermore, at the basin scale, return levels calculated from $elev^{coupled}$, other than $elev^{0.2H_s}$, display different spatial patterns. The 100-year return levels for elev^{coupled} are generally equal or higher than those derived from empirical approaches in the coastal regions where the conditions for the numerical model to accurately capture the wave setup development are met. These conditions imply the presence of energetic waves (high H_s and T_n) where coastal depth does not reach low enough values for waves to break in the model, and sufficient spatial resolution to resolve wave transformation processes. In regions characterized by wide and shallow continental shelves (e.g. gulfs of Valencia, Gabes and Syrte), 100-year elev^{coupled} return levels often exceed those produced by other methods based on Stockdon et al. (2006) formulation. Conversely, in the absence of a continental platform, hydrodynamic-wave coupled numerical models are prone to underestimating the wave setup contribution, due to the insufficient spatial resolution near the coast (Nayak et al., 2012; Martín et al., 2023). To illustrate this point, the local investigation carried out in PDP (Section 4) showed differences in wave setup between a regional and a local approach, that are attributed solely to the difference in the grid resolution. In addition to the grid node density, that plays a pivotal role when employing a 2DH approach, other factors in the modeling configuration also impact the wave setup, as explained in the introduction. Indeed, though a 3D simulation at such spatial and temporal scales is not conceivable, Martins et al. (2022) showed, for 2DH approaches, the benefit from using a vortex force formalism compared to a radiation stress formalism, especially in the case of a steep bottom. As a comparable analysis can be conducted in PDP that is characterized by a mild slope of 0.027, additional investigations could be undertaken to evaluate the influence of VF formalism on the magnitude of wave setup contributions at a larger spatial scale such as the Mediterranean. Despite the substantial dispersion in results observed among various commonly employed approaches (empirical, semi-empirical, and numerical) for estimating wave setup and the limitations associated, our work confirms that the wave setup contribution to extreme sea levels in many parts of the Mediterranean coasts is non negligible and should be accounted for. We found that in the Mediterranean basin, the wave setup component represents more than 20% of extreme sea levels for $elev^{coupled}$ and $elev^{\beta_{0.04}}$ 100-year return level at 13.1% and 6.6% of coastal points, respectively.

In conclusion, this work underscores the importance of incorporating wave setup estimation in coastal hazards assessment and advocates for its inclusion, whenever feasible. The findings presented in this research demonstrate that including this phenomenon can substantially alter storm surge levels. For instance, as initially highlighted in Toomey et al. (2022a), it has been shown along the coasts of the Gulf of Valencia, an extreme sea level of 46 cm corresponding to a return period of 100 years is expected to occur every 8 years when accounting for wave setup. This study also shows that the wave setup representation through numerical modeling at regional or global scale is overall very limited, with a largely underestimated contribution to extreme sea levels in most parts of the Mediterranean. Consequently, outputs from numerical modeling such as the CoExMed dataset should be regarded as conservative lower limit for regional assessment of the wave setup contribution to coastal extreme sea level. On the other hand, wave setup estimation from formulations like the one proposed by Stockdon et al. (2006) provides levels for the wave runup, but can yield very variable results depending on local wave inputs and morphological parameters. Designed and validated at local scale, for sandy beach application and during moderate wave conditions, such formulation should be applied with caution when used at regional or global scale. Extracting wave setup component from such methodologies proves difficult because of the absence of global or regional database of local beach-face slope, that can strongly change over time especially where the wave regime has a strong seasonality. Note that the latter is also a limitation for numerical models using time-invariant bathymetry. Furthermore, uncertainties from methods found in the literature are multiple, and as mentioned earlier, can lead to very disperse results with poor confidence. As performed in Melet et al. (2020), with the collection of local beach slope information at 308 different location around the world, we recommend the application of empirical formulation for regional and global studies at specific sites, or relatively large areas showing very similar morphological characteristics and wave climate, and certainly not continuously for the worldwide coastlines.

Funding

This study was supported by the project PID2021-124085OB-I00 and PID2021-123352OB-C31 both funded by MCIN/AEI/10.13039/501100011033/FEDER, UE). T.T acknowledges an FPI, USA grant associated with the MOCCA project (grant number PRE2019-088046). T.W. acknowledges support by the National Science Foundation, USA (grant number 2141461) and NASA's Sea Level Change Team, USA (grant number 80NSSC20K1241). A.E. was funded by Marie Skłodowska-Curie Actions, USA, project 101019470 – SpaDeRisks. A.A. was funded by the Conselleria d'Educació, Universitat i Recerca del Govern Balear, Spain through the Direcció General de Política Universitària i Recerca and by the Fondo Social Europeo, Spain for the period 2014–2020 (grant no. PD/011/2019). The present research was carried out in the framework of the AEI accreditation "Maria de Maeztu Centre of Excellence" given to IMEDEA (CSIC-UIB), Spain (CEX2021-001198).

CRediT authorship contribution statement

Tim Toomey: Conceptualization, Data curation, Formal analysis, Investigation, Methodology, Software, Validation, Visualization, Writing – original draft. Marta Marcos: Conceptualization, Funding acquisition, Investigation, Methodology, Resources, Validation, Writing – review & editing, Supervision. Thomas Wahl: Conceptualization, Investigation, Methodology, Supervision, Validation, Writing – review & editing. Miguel Agulles: Data curation, Formal analysis, Investigation, Methodology, Software, Validation, Writing – review & editing, Supervision. Alejandra R. Enríquez: Investigation, Methodology, Supervision, Validation, Writing – review & editing. Angel Amores: Methodology, Software, Supervision, Validation, Writing – review & editing. Alejandro Orfila: Supervision, Validation, Writing – review & editing.

Declaration of competing interest

The authors declare that they have no known competing financial interests or personal relationships that could have appeared to influence the work reported in this paper.

Data availability

Data will be made available on request.

Appendix A. Supplementary data

Supplementary material related to this article can be found online at https://doi.org/10.1016/j.wace.2024.100685.

References

Abessolo, G.O., Birol, F., Almar, R., Léger, F., Bergsma, E., Brodie, K., Holman, R., 2023. Wave influence on altimetry sea level at the coast. Coast. Eng. 180, 104275. http://dx.doi.org/10.1016/j.coastaleng.2022.104275, URL https://www.sciencedirect.com/science/article/pii/S0378383922001880.

Agulles, M., Jordà, G., 2023. Quantification of error sources in wave runup estimates on two mediterranean sandy beaches. Coast. Eng. 104402. http://dx.doi.org/10.1016/j.coastaleng.2023.104402, URL https://www.sciencedirect.com/science/article/pii/S0378383923001266.

Agulles, M., Jordà, G., Lionello, P., 2021. Flooding of sandy beaches in a changing climate. The case of the balearic islands (NW mediterranean). Front. Mar. Sci. 8, http://dx.doi.org/10.3389/fmars.2021.760725, URL https://www.frontiersin.org/articles/10.3389/fmars.2021.760725.

Almar, R., Ranasinghe, R., Bergsma, E.W.J., Diaz, H., Melet, A., Papa, F., Vousdoukas, M., Athanasiou, P., Dada, O., Almeida, L.P., Kestenare, E., 2021. A global analysis of extreme coastal water levels with implications for potential coastal overtopping. Nature Commun. 12 (1), 3775. http://dx.doi.org/10.1038/s41467-021-24008-9.

- Amores, A., Marcos, M., Carrió, D.S., Gómez-Pujol, L., 2020. Coastal impacts of storm gloria (january 2020) over the north-western mediterranean. Nat. Hazards Earth Syst. Sci. 20 (7), 1955–1968. http://dx.doi.org/10.5194/nhess-20-1955-2020, URL https://nhess.copernicus.org/articles/20/1955/2020/.
- Apotsos, A., Raubenheimer, B., Elgar, S., Guza, R.T., Smith, J.A., 2007. Effects of wave rollers and bottom stress on wave setup. J. Geophys. Res.: Oceans 112 (C2), http://dx.doi.org/10.1029/2006JC003549, arXiv:https://agupubs.onlinelibrary.wiley.com/doi/pdf/10.1029/2006JC003549, URL https://agupubs.onlinelibrary.wiley.com/doi/abs/10.1029/2006JC003549.
- Army Corps of Engineers, U.S., 1984. Shore Protection Manual, 4th Washington DC, U.S. Govt.
- Atkinson, A.L., Power, H.E., Moura, T., Hammond, T., Callaghan, D.P., Baldock, T.E., 2017. Assessment of runup predictions by empirical models on non-truncated beaches on the south-east Australian coast. Coast. Eng. 119, 15–31. http://dx.doi.org/10.1016/j.coastaleng.2016.10.001, URL https://www.sciencedirect.com/science/article/pii/S037838391630285X.
- Bathymetry, C.E., 2018. EMODnet bathymetry consortium (2018). EMODnet digital bathymetry (DTM 2018). EMODnet bathymetry consortium. http://dx.doi.org/10. 12770/18ff0d48-b203-4a65-94a9-5fd8b0ec35f6.
- Bennis, A.C., Ardhuin, F., Dumas, F., 2011. On the coupling of wave and three-dimensional circulation models: Choice of theoretical framework, practical implementation and adiabatic tests. Ocean Model. 40 (3), 260–272. http://dx.doi.org/10.1016/j.ocemod.2011.09.003, URL https://www.sciencedirect.com/science/article/pii/S1463500311001570.
- Bennis, A.C., Dumas, F., Ardhuin, F., Blanke, B., 2014. Mixing parameterization: Impacts on rip currents and wave set-up. Ocean Eng. 84, 213–227. http://dx.doi.org/10.1016/j.oceaneng.2014.04.021, URL https://www.sciencedirect.com/science/article/pii/S0029801814001607.
- Bernabéu, A., Medina, R., Vida, C., Muñoz-Pérez, J., 2001. Estudio morfológico del perfil de playa: modelo de perfil de equilibrio en dos tramos.. Rev. Sociedad Geológica de España (14), 227–236.
- Bertin, X., Li, K., Roland, A., Bidlot, J., 2015. The contribution of short-waves in storm surges: Two case studies in the bay of biscay. Cont. Shelf Res. 96, http://dx.doi.org/10.1016/j.csr.2015.01.005.
- Buckley, M.L., Lowe, R.J., Hansen, J.E., Dongeren, A.R.V., 2016. Wave setup over a fringing reef with large bottom roughness. J. Phys. Oceanogr. 46 (8), 2317– 2333. http://dx.doi.org/10.1175/JPO-D-15-0148.1, URL https://journals.ametsoc. org/view/journals/phoc/46/8/jpo-d-15-0148.1.xml.
- Camus, P., Mendez, F.J., Medina, R., Cofiño, A.S., 2011. Analysis of clustering and selection algorithms for the study of multivariate wave climate. Coast. Eng. 58 (6), 453–462. http://dx.doi.org/10.1016/j.coastaleng.2011.02.003, URL https://www. sciencedirect.com/science/article/pii/S0378383911000354.
- Cid, A., Menendez, M., Castanedo, S., Abascal, A., Mendez, F., Medina, R., 2015. Long-term changes in the frequency, intensity and duration of extreme storm surge events in southern Europe. Clim. Dyn. 46, http://dx.doi.org/10.1007/s00382-015-2659-1.
- Coles, S., 2001. An introduction to statistical modeling of extreme values. In: Springer Series in Statistics, Springer-Verlag, London.
- Corps of Engineers, U.A., 2002. Coastal Engineering Manual. U.S. Army Corps of Engineers Washington, D.C., Washington, D.C..
- Dee, D.P., Uppala, S.M., Simmons, A.J., Berrisford, P., Poli, P., Kobayashi, S., Andrae, U., Balmaseda, M.A., Balsamo, G., Bauer, P., Bechtold, P., Beljaars, A.C.M., van de Berg, L., Bidlot, J., Bormann, N., Delsol, C., Dragani, R., Fuentes, M., Geer, A.J., Haimberger, L., Healy, S.B., Hersbach, H., Hólm, E.V., Isaksen, L., K° allberg, P., Köhler, M., Matricardi, M., McNally, A.P., Monge-Sanz, B.M., Morcrette, J.J., Park, B.K., Peubey, C., de Rosnay, P., Tavolato, C., Thépaut, J.N., Vitart, F., 2011. The ERA-interim reanalysis: configuration and performance of the data assimilation system. Q. J. R. Meteorol. Soc. 137 (656), 553–597. http://dx.doi.org/10.1002/qj.828, arXiv:https://rmets.onlinelibrary.wiley.com/doi/abs/10.1002/qj.828.
- Diaz, H., Almar, R., Bergsma, E.W.J., Leger, F., 2019. On the use of satellite-based digital elevation models to determine coastal topography. In: IGARSS 2019 - 2019 IEEE International Geoscience and Remote Sensing Symposium. pp. 8201–8204. http://dx.doi.org/10.1109/IGARSS.2019.8899189.
- Fenton, J., McKee, W., 1990. On calculating the lengths of water waves. Coast. Eng. 14 (6), 499–513. http://dx.doi.org/10.1016/0378-3839(90)90032-R, URL https://www.sciencedirect.com/science/article/pii/037838399090032R.
- Fernández-Montblanc, T., Vousdoukas, M., Mentaschi, L., Ciavola, P., 2020. A Pan-European high resolution storm surge hindcast. Environ. Int. 135, 105367. http: //dx.doi.org/10.1016/j.envint.2019.105367, URL https://www.sciencedirect.com/ science/article/pii/S0160412019324055.
- Fritz, H.M., Blount, C., Sokoloski, R., Singleton, J., Fuggle, A., McAdoo, B.G., Moore, A., Grass, C., Tate, B., 2007. Hurricane Katrina storm surge distribution and field observations on the Mississippi barrier islands. Estuar. Coast. Shelf Sci. 74 (1), 12–20. http://dx.doi.org/10.1016/j.ecss.2007.03.015, URL https://www.sciencedirect.com/science/article/pii/S0272771407000868.
- Guérin, T., Bertin, X., Coulombier, T., de Bakker, A., 2018. Impacts of wave-induced circulation in the surf zone on wave setup. Ocean Model. 123, 86–97. http://dx.doi.org/10.1016/j.ocemod.2018.01.006, URL https://www.sciencedirect.com/science/article/pii/S1463500318300246.

- Guza, R.T., Thornton, E.B., 1981. Wave set-up on a natural beach. J. Geophys. Res.: Oceans 86 (C5), 4133–4137. http://dx.doi.org/10.1029/JC086iC05p04133, arXiv: https://agupubs.onlinelibrary.wiley.com/doi/pdf/10.1029/JC086iC05p04133, URL https://agupubs.onlinelibrary.wiley.com/doi/abs/10.1029/JC086iC05p04133.
- Hemer, M.A., Trenham, C.E., 2016. Evaluation of a CMIP5 derived dynamical global wind wave climate model ensemble. Ocean Model. 103, 190–203. http://dx.doi. org/10.1016/j.ocemod.2015.10.009, URL https://www.sciencedirect.com/science/ article/pii/S1463500315002127, Waves and coastal, regional and global processes.
- Hersbach, H., Bell, B., Berrisford, P., Hirahara, S., Horányi, A., Muñoz-Sabater, J., Nicolas, J., Peubey, C., Radu, R., Schepers, D., Simmons, A., Soci, C., Abdalla, S., Abellan, X., Balsamo, G., Bechtold, P., Biavati, G., Bidlot, J., Bonavita, M., De Chiara, G., Dahlgren, P., Dee, D., Diamantakis, M., Dragani, R., Flemming, J., Forbes, R., Fuentes, M., Geer, A., Haimberger, L., Healy, S., Hogan, R.J., Hólm, E., Janisková, M., Keeley, S., Laloyaux, P., Lopez, P., Lupu, C., Radnoti, G., de Rosnay, P., Rozum, I., Vamborg, F., Villaume, S., Thépaut, J.N., 2020. The ERA5 global reanalysis. Q. J. R. Meteorol. Soc. 146 (730), 1999–2049. http://dx.doi.org/10.1002/qj.3803, arXiv:https://rmets.onlinelibrary.wiley.com/doi/abs/10.1002/qj.3803.
- Holthuijsen, L.H., 2007. Waves in Oceanic and Coastal Waters. Cambridge University Press, http://dx.doi.org/10.1017/CBO9780511618536.
- Infantes, E., Orfila, A., Simarro, G., Terrados, J., Luhar, M., Nepf, H., 2012. Effect of a seagrass (Posidonia oceanica) meadow on wave propagation. Mar. Ecol. Prog. Ser. 456, 63–72. http://dx.doi.org/10.3354/meps09754, URL https://www.int-res.com/abstracts/meps/v456/p63-72/.
- Kennedy, A.B., Westerink, J.J., Smith, J.M., Hope, M.E., Hartman, M., Taflanidis, A.A., Tanaka, S., Westerink, H., Cheung, K.F., Smith, T., Hamann, M., Minamide, M., Ota, A., Dawson, C., 2012. Tropical cyclone inundation potential on the Hawaiian Islands of Oahu and Kauai. Ocean Model. 52–53, 54–68. http://dx.doi.org/10.1016/j.ocemod.2012.04.009, URL https://www.sciencedirect.com/science/article/pii/\$11463500312000698.
- Kirezci, E., Young, I.R., Ranasinghe, R., Lincke, D., Hinkel, J., 2023. Global-scale analysis of socioeconomic impacts of coastal flooding over the 21st century. Front. Mar. Sci. 9, http://dx.doi.org/10.3389/fmars.2022.1024111, URL https://www. frontiersin.org/articles/10.3389/fmars.2022.1024111.
- Kirezci, E., Young, I., Ranasinghe, R., Muis, S., Nicholls, R., Lincke, D., Hinkel, J., 2020. Projections of global-scale extreme sea levels and resulting episodic coastal flooding over the 21st century. Sci. Rep. 10, 11629. http://dx.doi.org/10.1038/s41598-020-67736-6.
- Lavaud, L., Bertin, X., Martins, K., Arnaud, G., Bouin, M.N., 2020. The contribution of short-wave breaking to storm surges: The case klaus in the southern bay of biscay. Ocean Model. 156, 101710. http://dx.doi.org/10.1016/j.ocemod.2020.101710, URL https://www.sciencedirect.com/science/article/pii/S1463500320302122.
- Longuet-Higgins, M., Stewart, R., 1964. Radiation stresses in water waves; A physical discussion, with applications. Deep Sea Res. Oceanogr. Abstr. 11 (4), 529–562. http://dx.doi.org/10.1016/0011-7471(64)90001-4, URL https://www.sciencedirect.com/science/article/pii/0011747164900014.
- Marcos, M., Rohmer, J., Vousdoukas, M.I., Mentaschi, L., Le Cozannet, G., Amores, A., 2019. Increased Extreme Coastal water levels due to the combined action of storm surges and wind waves. Geophys. Res. Lett. 46 (8), 4356–4364. http://dx.doi.org/10.1029/2019GL082599, arXiv:https://agupubs.onlinelibrary.wiley.com/doi/pdf/10.1029/2019GL082599, URL https://agupubs.onlinelibrary.wiley.com/doi/abs/10.1029/2019GL082599.
- Marcos, M., Tsimplis, M.N., Shaw, A.G.P., 2009. Sea level extremes in southern Europe.
 J. Geophys. Res.: Oceans 114 (C1), http://dx.doi.org/10.1029/2008JC004912,
 arXiv:https://agupubs.onlinelibrary.wiley.com/doi/pdf/10.1029/2008JC004912,
 URL https://agupubs.onlinelibrary.wiley.com/doi/abs/10.1029/2008JC004912.
- Martín, A., Amores, A., Orfila, A., Toomey, T., Marcos, M., 2023. Coastal extreme sea levels in the caribbean sea induced by tropical cyclones. Nat. Hazards Earth Syst. Sci. 23 (2), 587–600. http://dx.doi.org/10.5194/nhess-23-587-2023, URL https://nhess.copernicus.org/articles/23/587/2023/.
- Martins, K., Bertin, X., Mengual, B., Pezerat, M., Lavaud, L., Guérin, T., Zhang, Y., 2022.
 Wave-induced mean currents and setup over barred and steep sandy beaches. Ocean Model. 179, 102110. http://dx.doi.org/10.1016/j.ocemod.2022.102110.
- Medugorac, I., Mirko, O., Ivica, J., Zoran, P., Miroslava, P., 2018. Adriatic storm surges and related cross-basin sea-level slope. J. Mar. Syst. 181, 79–90. http: //dx.doi.org/10.1016/j.jmarsys.2018.02.005, URL https://www.sciencedirect.com/ science/article/pii/S0924796317302701.
- Melet, A., Almar, R., Hemer, M., Le Cozannet, G., Meyssignac, B., Ruggiero, P., 2020. Contribution of wave setup to Projected Coastal sea level changes. J. Geophys. Res.: Oceans 125 (8), http://dx.doi.org/10.1029/2020JC016078, e2020JC016078, arXiv:https://agupubs.onlinelibrary.wiley.com/doi/pdf/10.1029/2020JC016078, URL https://agupubs.onlinelibrary.wiley.com/doi/abs/10.1029/2020JC016078, e2020JC016078 2020JC016078.
- Melet, A., Meyssignac, B., ans G. Le Cozannet, R.A., 2018. Under-estimated wave contribution to coastal sea-level rise. Nature Clim. Change 8, http://dx.doi.org/ 10.1038/s41558-018-0088-y.
- Mentaschi, L., Vousdoukas, M., Fernández-Montblanc, T., Kakoulaki, G., Voukouvalas, E., Besio, G., Salamon, P., 2020. Assessment of Global Wave Models on Regular and Unstructured Grids Using the Unresolved Obstacles Source Term. Springer, Heidelberg, http://dx.doi.org/10.1007/s10236-020-01410-3, URL http://hdl.handle.net/10498/23920.

- Muis, S., Apecechea, M.I., Dullaart, J., de Lima Rego, J., Madsen, K.S., Su, J., Yan, K., Verlaan, M., 2020. A high-resolution global dataset of extreme sea levels, tides, and storm surges, including future projections. Front. Mar. Sci. 7, 263. http://dx.doi.org/10.3389/fmars.2020.00263, URL https://www.frontiersin.org/article/10.3389/fmars.2020.00263
- Nayak, S., Bhaskaran, P.K., Venkatesan, R., 2012. Near-shore wave induced setup along kalpakkam coast during an extreme cyclone event in the Bay of Bengal. Ocean Eng. 55, 52–61. http://dx.doi.org/10.1016/j.oceaneng.2012.07.036, URL https://www.sciencedirect.com/science/article/pii/S0029801812002910.
- Pedreros, R., Idier, D., Muller, H., Lecacheux, S., Paris, F., Yates, M., Dumas, F., Pineau-Guillou, L., Senechal, N., 2018. Relative contribution of wave setup to the storm surge: Observations and modeling based analysis in open and protected environments (Truc Vert beach and Tubuai island). J. Coast. Res. 85, 1046–1050. http://dx.doi.org/10.2112/S185-210.1.
- Pérez-Gómez, B., García-León, M., García-Valdecasas, J., Clementi, E., Mösso Aranda, C., Pérez-Rubio, S., Masina, S., Coppini, G., Molina-Sánchez, R., Muñoz-Cubillo, A., García Fletcher, A., Sánchez González, J.F., Sánchez-Arcilla, A., Álvarez Fanjul, E., 2021. Understanding sea level processes during western mediterranean storm gloria. Front. Mar. Sci. 8, http://dx.doi.org/10.3389/fmars.2021.647437, URL https://www.frontiersin.org/article/10.3389/fmars.2021.647437.
- Pineau-Guillou, L., Bouin, M.N., Ardhuin, F., Lyard, F., Bidlot, J.R., Chapron, B., 2020. Impact of wave-dependent stress on storm surge simulations in the north sea: Ocean model evaluation against in situ and satellite observations. Ocean Model. 154, 101694. http://dx.doi.org/10.1016/j.ocemod.2020.101694, URL https://www.sciencedirect.com/science/article/pii/S1463500320301967.
- Pond, Pickard, 2013. Introductory Dynamical Oceanography, 2nd edition Oxford: Butterworth-Heinemann.
- Raubenheimer, B., Guza, R.T., Elgar, S., 2001. Field observations of wave-driven setdown and setup. J. Geophys. Res.: Oceans 106 (C3), 4629-4638. http://dx.doi.org/10.1029/2000JC000572, arXiv:https://agupubs.onlinelibrary. wiley.com/doi/pdf/10.1029/2000JC000572. URL https://agupubs.onlinelibrary. wiley.com/doi/abs/10.1029/2000JC000572.
- Ray, R.D., Merrifield, M.A., Woodworth, P.L., 2022. Wave setup at the Minamitorishima tide gauge. J. Oceanogr. 79 (1), 13–26. http://dx.doi.org/10.1007/s10872-022-00659-0
- Roelvink, D.J., van Dongeren, A., McCall, R., Hoonhout, B., van Rooijen, A., van Geer, P., de Vet, L., Nederhoff, K., Quataert, E., 2015. Xbeach technical reference: Kingsday release. http://dx.doi.org/10.13140/RG.2.1.4025.6244.
- Roland, A., Cucco, A., Ferrarin, C., Hsu, T.W., Liau, J.M., Ou, S.H., Umgiesser, G., Zanke, U., 2009. On the development and verification of a 2-D coupled wavecurrent model on unstructured meshes. J. Mar. Syst. 78, S244–S254. http://dx.doi.org/10.1016/j.jmarsys.2009.01.026, URL https://www.sciencedirect.com/science/article/pii/S0924796309001535, Coastal Processes: Challenges for Monitoring and Prediction.
- Rueda, A., Vitousek, S., Camus, P., Tomás, A., Espejo, A., Losada, I.J., Barnard, P.L., Erikson, L.H., Ruggiero, P., Reguero, B.G., Mendez, F.J., 2017. A global classification of coastal flood hazard climates associated with large-scale oceanographic forcing. Sci. Rep. 7 (1), 5038.
- Ruiz-Fernández, J.M., Guillén, J., Ramos-Segura, A., Otero, M., Tello-Antón, M.O., Mateo, M., Bernardeau-Esteller, J., Rueda, J.L., Urra, J., Mateo, A., Ballesteros-Fernández, E., Templado, J., Romero, J., Rodríguez, M.P., Alcoverro, T., de Torres, M., Manzanera, M., Allué, R., Álvarez, E., Jofre, A.M.G., Marbà, N., Carreras, D., Sánchez-Lizaso, J.L., Fernández-Torquemada, Y., Triviño, A., Jiménnez, S., Martínez, J., Gras, D., Soler, G., Marín-Guirao, L., del Rocío García-Muñoz, M., María-Dolores, E., Guirao, J., Baraza, F., López, A., García, C., Arroyo, M., Brun, Barrajón, A., Brun, F., del Castillo, F., de-la Rosa, J., Almela, E., Fernández, M., Hernández, I., Moreno, D., Pérez, J.L., Remón, J., Vergara, J., Soledad, M., Zapata, F., Martínez, F., Orozco, A., Villalón, J., de la Rosa, M.R., Tuya, F., Herrera, R., Moro, L., Espino, F., Haroun, R., Sintes, P.M., Cacabelos, E., Quintas, P., Troncoso, J., Sánchez, J., Amigo, J., Romero, I., García, V., Cremades, J., Bárbara, I., Bueno, Á., Fernández, J., Peón, P., García, S., Sánchez, T., Vázquez, V., Ondiviela, B., García, G., Recio, M., Puente, A., Juanes, J., Garmendia, J., Chust, G., Borja, Á., Franco, J., 2015. Atlas de las praderas marinas de España.
- Sánchez-Artús, X., Gracia, V., Espino, M., Sierra, J.P., Pinyol, J., Sánchez-Arcilla, A., 2023. Present and future flooding and erosion along the NW spanish Mediterranean Coast. Front. Mar. Sci. 10.

- Stockdon, H., Holman, R., Howd, P., Sallenger, A., 2006. Empirical parameterization of setup, swash, and runup. Coast. Eng. 53, 573–588. http://dx.doi.org/10.1016/j. coastaleng.2005.12.005.
- Stockdon, H., Thompson, D., Plant, N., Long, J., 2014. Evaluation of wave runup predictions from numerical and parametric models. Coast. Eng. 92, 1–11. http://dx.doi.org/10.1016/j.coastaleng.2014.06.004, URL https://www.sciencedirect.com/science/article/pii/S0378383914001239.
- Sunamurra, T., 1984. Quantitative predictions of beach-face slopes. GSA Bull. 95 (2), 242–245. http://dx.doi.org/10.1130/0016-7606(1984)95<242:QPOBS>2.0.CO;2, arXiv:https://pubs.geoscienceworld.org/gsa/gsabulletin/article-pdf/95/2/242/3434635/i0016-7606-95-2-242.pdf.
- Tadono, T., Nagai, H., Ishida, H., Oda, F., Naito, S., Minakawa, K., Iwamoto, H., 2016. Generation of the 30 M-Mesh global digital surface model by alos prism. Int. Arch. Photogramm., Remote Sens. Spatial Inf. Sci. XLI-B4, 157–162. http://dx.doi.org/10.5194/isprs-archives-XLI-B4-157-2016, URL https://www.int-arch-photogramm-remote-sens-spatial-inf-sci.net/XLI-B4/157/2016/.
- Thompson, P., Cai, Y., Reeve, D., Stander, J., 2009. Automated threshold selection methods for extreme wave analysis. Coast. Eng. 56 (10), 1013–1021. http:// dx.doi.org/10.1016/j.coastaleng.2009.06.003, URL https://www.sciencedirect.com/ science/article/pii/S0378383909000921.
- Tintoré, J., Vizoso, G., Casas, B., Heslop, E., Pascual, A., Orfila, A., Ruiz, S., Martínez-Ledesma, M., Torner, M., Cusí, S., Diedrich, A., Balaguer, P., Gómez-Pujol, L., Álvarez-Ellacuria, A., Gómara, S., Sebastian, K., Lora, S., Beltrán, J.P., Renault, L., Juzá, M., Álvarez, D., March, D., Garau, B., Castilla, C., Cañellas, T., Roque, D., Lizarán, I., Pitarch, S., Carrasco, M.A., Lana, A., Mason, E., Escudier, R., Conti, D., Sayol, J.M., Barceló, B., Alemany, F., Reglero, P., Massuti, E., Vélez-Belchí, P., Ruiz, J., Oguz, T., Gómez, M., Álvarez, E., Ansorena, L., Manriquez, M., 2013. SOCIB: The balearic Islands Coastal ocean observing and forecasting system responding to science, technology and society needs. Mar. Technol. Soc. J. 47 (1), 101–117. http://dx.doi.org/10.4031/MTSJ.47.1.10, URL https://www.ingentaconnect.com/content/mts/mts/2013/00000047/00000001/art00010.
- Toomey, T., Amores, A., Marcos, M., Orfila, A., 2022a. Coastal sea levels and windwaves in the mediterranean sea since 1950 from a high-resolution ocean reanalysis.

 Front. Mar. Sci. 9, http://dx.doi.org/10.3389/fmars.2022.991504, URL https://www.frontiersin.org/articles/10.3389/fmars.2022.991504.
- Toomey, T., Amores, A., Marcos, M., Orfila, A., Romero, R., 2022b. Coastal hazards of tropical-like cyclones over the mediterranean sea. J. Geophys. Res.: Oceans 127 (2), http://dx.doi.org/10.1029/2021JC017964, e2021JC017964, arXiv:https://agupubs.onlinelibrary.wiley.com/doi/pdf/10.1029/2021JC017964, URL https://agupubs.onlinelibrary.wiley.com/doi/abs/10.1029/2021JC017964, e2021JC017964 2021JC017964.
- Vitousek, S., Barnard, P.L., Fletcher, C.H., Frazer, N., Erikson, L., Storlazzi, C.D., 2017.

 Doubling of coastal flooding frequency within decades due to sea-level rise. Sci. Rep. 7 (1), 1399. http://dx.doi.org/10.1038/s41598-017-01362-7.
- Vousdoukas, M.I., Mentaschi, L., Voukouvalas, E., Verlaan, M., Feyen, L., 2017. Extreme sea levels on the rise along Europe's coasts. Earth's Future 5 (3), 304–323. http://dx.doi.org/10.1002/2016EF000505, arXiv:https://agupubs.onlinelibrary.wiley.com/doi/pdf/10.1002/2016EF000505, URL https://agupubs.onlinelibrary.wiley.com/doi/abs/10.1002/2016EF000505.
- Vousdoukas, M., Voukouvalas, E., Annunziato, A., Giardino, A., Feyen, L., 2016.

 Projections of extreme storm surge levels along Europe. Clim. Dyn. 47, http://dx.doi.org/10.1007/s00382-016-3019-5.
- Wahl, T., Haigh, I., Nicholls, R., Arns, A., Dangendorf, S., Hinkel, J., Slangen, A., 2017.
 Understanding extreme sea levels for broad-scale coastal impact and adaptation analysis. Nature Commun. 8, 16075. http://dx.doi.org/10.1038/ncomms16075.
- Wang, D.P., Oey, L.Y., 2008. Hindcast of waves and currents in Hurricane Katrina. Bull. Am. Meteorol. Soc. 89 (4), 487–496. http://dx.doi.org/10.1175/BAMS-89-4-487, URL https://journals.ametsoc.org/view/journals/bams/89/4/bams-89-4-487.xml.
- Wessel, P., Smith, W., 1996. A global self-consistent, hierarchical, high-resolution shoreline. J. Geophys. Res. 101, 8741–8743.
- Wolff, C., Vafeidis, A.T., Muis, S., Lincke, D., Satta, A., Lionello, P., Jimenez, J.A., Conte, D., Hinkel, J., 2018. A mediterranean coastal database for assessing the impacts of sea-level rise and associated hazards. Sci. Data 5 (1), 180044. http: //dx.doi.org/10.1038/sdata.2018.44.
- Zhang, Y.J., Ye, F., Stanev, E.V., Grashorn, S., 2016. Seamless cross-scale modeling with SCHISM. Ocean Model. 102, 64–81. http://dx.doi.org/10.1016/j.ocemod.2016.05. 002.